SOLID-STATE THERMAL AND PHOTOCHEMICAL REACTION KINETICS

by

EUGENE LYNN SIMMONS, B. S., M. S.

A DISSERTATION

IN

CHEMISTRY

Submitted to the Graduate Faculty
of Texas Technological College
in Partial Fulfillment of
the Requirements for
the Degree of

DOCTOR OF PHILOSOPHY

AC
801
T3
1968
No.2
cop.2

ACKNOWLEDGMENTS

I would like to express my appreciation to Dr. A. L. Draper for his direction of this work and to the other members of my committee, Dr. Joe Dennis, Dr. R. E. Wilde, Dr. R. J. Thompson, and Dr. Gordon Fuller.

I would like to thank the National Aeronautics and Space Administration for their financial support of a large part of this research.

I would also like to acknowledge the loan of a magnet and an Hitachi spectrophotometer by Dr. R. J. Thompson purchased by the R. A. Welch Foundation, Grant D-097, and the loan of a reflectance spectrometer by Dr. W. W. Wendlandt purchased by the Airforce Office of Molecular Research.

TABLE OF CONTENTS

Page

LIST OF TABLES

LIST OF FIGURES

Figure Page

CHAPTER I

STATEMENT OF THE PROBLEM

For a long time certain transition-metal coordination compounds have been known to undergo chemical reactions when heated or irradiated with ultraviolet radiation. Although the kinetics of many of these reactions have been investigated in aqueous solutions, few have been investigated in the solid state. In fact, few solid-state photochemical kinetic investigations of any reactions have been carried out. Consequently, very little is known concerning the photochemical reaction kinetics of a powdered sample.

Solid-state photochemical kinetic investigators are confronted with many problems which do not arise in the corresponding solution photochemical kinetics. Since a solid-state photochemical reaction involves only the immediate surface of a sample, it is very difficult to measure the amount of sample reacted. In fact, the amount reacted varies with depth into the sample, for solids not only absorb radiation but also reflect it, thereby decreasing the radiation intensity penetrating the sample. Furthermore, two types of reflection occur upon the irradiation of a powdered sample (diffuse and regular or surface reflection). This greatly complicates the development of a theoretical reaction-rate equation. Many

powdered solid samples undergo a change in volume during a chemical reaction. The concentration of the reactant therefore cannot be reliably expressed in the usual units of moles per unit volume.

As yet, these problems have not been solved and a suitable theoretical expression for the rate of a solid-state photochemical reaction has not been developed. The dependence of the rate of such a reaction on the amount reacted, the intensity and wavelength of the radiation, and the depth into the sample are not known.

Few solid-state thermal reaction kinetic studies in the past have yielded information which make possible the formulation of a chemical reaction mechanism. Physical and geometric properties play such an important role in controlling solid-state thermal reaction that chemical processes are often undetectable in kinetic studies.

Although the solid-state thermal reactions of many transition metal coordination compounds have been extensively investigated, very little is known concerning their reaction mechanisms. The kinetics of such reactions in the past have been explained on the basis of nucleus formation, diffusion, and other physical processes. Consequently, little is known concerning the chemical nature of solid-state reactions of transition metal coordination compounds.

An attempt is made in this investigation to solve some of the problems involved in solid-state thermal and photochemical reaction kinetics so that meaningful data can be obtained from which chemical mechanisms can be postulated. The dependence of the rate of a solid-state photochemical reaction on the amount of sample reacted

and the intensity of the radiation is derived on a theoretical basis and the results are tested experimentally. The dependence of the rate of such a reaction on the wavelength of the radiation is determined experimentally and an attempt is made to explain the results at least qualitatively. Then, the data obtained from a solid-state photochemical reaction are compared with those obtained from the same reaction carried out thermally in order to postulate a chemical reaction mechanism.

In order to carry out this investigation, a compound which undergoes the same reaction photochemically and thermally was necessary. An example of such a compound is potassium tris(oxalato)-manganate(III) 3-hydrate. The photochemical and the thermal reactions of this compound have been thoroughly investigated in aqueous solutions and have been found to proceed by similar mechanisms. It has also been found to yield the same products photochemically and thermally in the solid state. It may then be expected that the solid-state reactions proceed by similar mechanisms. Also, the reactions of this compound represent an important type of reaction of transition-metal coordination compounds. These are oxidation-reduction reactions. It is hoped that a better understanding of the solid-state reactions of this compound will give an insight into the chemistry of all reactions of this type.

CHAPTER II

SURVEY OF THE LITERATURE

Photochemistry is basically the study of the effects of electromagnetic radiation upon a chemical system. Probably the first work which could be called photochemistry occurred in the early 1700's. It was not until 1817, however, that the first law of photochemistry was stated by Grotthus. This law states that only light which is absorbed by a system can cause a chemical reaction. It was later found by Draper that the rate of a reaction is proportional to the intensity of the light used (1, 2).

After Planck introduced the idea of the quantum, Stark (3, 4) and later Einstein (5, 6) introduced the idea that one quantum of radiation is absorbed for each molecule which is excited. This is known as Einstein's equivalence law. The equivalence law introduces the quantum yield, which is defined as the number of reactant molecules which react after the absorption of one photon of radiation. The quantum yield is an important number in photochemistry, and it can tell much about the mechanism of a reaction. From the theory of the interaction of radiation with a gaseous or a liquid chemical system that has been developed, the rate equation for a chemical reaction has been derived (7).

Because of the recent development of the technique of reflectance

spectroscopy, several equations have been derived which describe the interaction of radiation on a powdered sample. The derivations have been reviewed by Wendlandt and Hecht (8). Probably the most important of the equations derived are those which treat diffusely reflected radiation by the introduction of a reflection coefficient.

The spectra of many transition-metal coordination compounds contain charge-transfer bands in the ultraviolet region. These bands are often caused by the excitation of ligand electrons into empty E_g metal orbitals (9). The effect of such a transition is to transfer an electron from the ligand to the metal ion. If a stable configuration results from such a transfer, the electron may remain in the E_g orbital, thereby reducing the metal ion. Photochemical oxidation-reduction reactions may therefore occur if a transition-metal coordination compound with an empty E_g orbital is irradiated by radiation whose wavelength corresponds to the energy of its charge-transfer band (10, 11).

There have been many attempts to explain solid-state thermal reaction kinetics on the basis of nucleus formation and growth and of diffusion of gases or reactive species through a sample. These attempts and the rate equations derived from them have been reviewed by Young (12) and by Garner (13). While these rate equations do apply to many solid-state reactions, they describe only physical processes, and, consequently, little information concerning the chemical nature of a sample can be obtained from their use, especially if rate controlling oxidation-reduction steps are involved.

There have been many investigations of solid-state thermal reactions of transition-metal coordination compounds. These investigations, however, were limited to the determination of reaction temperatures and stoichiometries. There have been a few investigations in which attempts were made to determine reaction mechanisms dependent on a chemical step such as an electron transfer. Attempts have been made to determine the chemical mechanisms of the solid-state thermal oxidation-reduction reactions of the compounds $Co[(NH_3)_6]X_3$ (X = Cl, Br) (14-17). Mechanisms have been postulated for the solid-state thermal ligand replacement reactions of the compounds, $[Cr(en)_3]X_3$ (X= Cl, Br, I, SCN, CN) (18). Also, possible mechanisms for the solid-state thermal oxidation-reduction reactions of the compounds, $K_3[M(C_2O_4)_3]\cdot 3H_2O$ (M = Mn, Co, Fe), have been suggested but without verification (19-22).

Unlike thermal reactions, photochemical reactions of transition-metal coordination compounds have not been extensively investigated. From the few investigations that have been carried out, there appear to be three types of solid-state photochemical reactions of transition-metal compounds. These are isomerization, ligand replacement, and oxidation-reduction reactions. There have been only one solid-state photochemical isomerization reaction (23) and one solid-state ligand replacement reaction (24) previously investigated.

By far the most numerous solid-state photochemical reactions of transition-metal compounds that have been studied are oxidation-reduction reactions. In every case investigated, the central metal

ion was reduced and a molecule, or an anion which was either in or outside of the coordination sphere, was oxidized. Because of their applications to photography, there has been a large number of studies of the solid-state photochemical oxidation-reduction reactions of the silver halides. Several investigations of the photochemical reductions of Hg(I) and Tl(I) in the compounds, HgN_3 and TlN_3, in the solid state have been reported (25-27). In these studies, the rates of the reactions as functions of the intensity and wavelength of the radiation and of the sample temperature were determined only in a qualitative manner. No solid-state photochemical rate equation was developed. The stoichiometries of the oxidation-reduction reactions of several Hg(II) compounds in the solid state have also been determined (28). The color changes involved in the solid-state photochemical oxidation-reduction reactions of the compounds, $K_3[Mn(C_2O_4)_3]\cdot 3H_2O$, $K_3[Co(C_2O_4)_3]\cdot 3H_2O$, and $K_3[Fe(C_2O_4)_3]\cdot 3H_2O$, have been observed (29, 30) and their reaction stoichiometries have been determined (19-22).

The oxalato complexes of manganese(III), cobalt(III), and iron-(III) have been of interest because they undergo similar reactions thermally and photochemically. Investigations of both the thermal and the photochemical reactions of these compounds have been carried out in aqueous solutions (31-40). In every case the central metal ion was reduced from the trivalent to the divalent state and an oxalat ligand was oxidized to carbon dioxide. For the reactions of all

three compounds, an oxalate ion radical was postulated as the electron transferring species.

In the solid state, the oxalato complexes of manganese(III), cobalt(III), and iron(III) yield different type thermal reaction products (19-22). Furthermore, the cobalt compound yields different products upon thermal reaction than upon photochemical reaction and there is still some uncertainty in the reaction stoichiometry of the thermal reaction of the iron compound. However, the manganese compound was found to give the same products during its thermal and photochemical reactions. The reaction proceeded as follows:

$$2K_3[Mn(C_2O_4)_3]\cdot 3H_2O \xrightarrow{\Delta \text{ or } h\nu} 2K_2[Mn(C_2O_4)_2] + K_2C_2O_4 + 2CO_2 + 6H_2O. \quad (1)$$

This reaction occurred at about 80° C and proceeded rapidly. It also proceeded rapidly upon irradiation with ultraviolet radiation from a mercury vapor light source.

As the literature survey above shows, there are still a number of unanswered questions concerning solid-state oxidation-reduction reactions of transition metal coordination compounds. The reaction given by Equation 1 appears to be suitable for an investigation comparing the thermal and photochemical reaction kinetics. Such an investigation was carried out and is presented in the following pages.

CHAPTER III

THEORETICAL DISCUSSION

A Photochemical Reaction Rate Equation

There has been no derivation of an equation describing the rate of the photochemical reaction of a powdered sample. Therefore, it was necessary to derive one in order to carry out this investigation. However, an equation describing the rate of a photochemical reaction of a fluid sample with slab geometry has previously been developed (7). This equation is

$$\text{average rate of reaction} = \frac{\phi I_o (1 - e^{-\epsilon[A]L})}{L h \nu} \qquad (2)$$

where ϕ is the quantum yield, I_o the initial intensity of the radiation, L the reaction cell length, $[A]$ the concentration of reactant, ν the frequency of the radiation, h Planck's constant, and ϵ the absorption coefficient. This equation, however, cannot be used for the study of a powdered sample. Therefore, a new equation was derived to describe the rate of the photochemical reaction of a powdered sample. The new equation was derived in a manner similar to that of Equation 2 except that modifications were made to account for the inhomogeneity of a solid-state reaction and for the reflected radiation.

A powdered sample of a reactant, R, reacts upon the absorption of a photon to give an excited species, R*, or

$$R + h\nu \longrightarrow R^* . \qquad (3)$$

The excited species may then react in some manner to yield one or more products, P. The number of resultant product molecules will later be taken into account by the introduction of the quantum yield.

After a sample of this powdered reactant has been irradiated with monochromatic radiation with an intensity, after surface reflection has taken place, of I_o' for a period of time, t, it will consist of a mixture of reactant and product. It contains [R] moles of reactant per unit volume and $R_o - [R]$ reacted per unit volume, where R_o is the initial concentration of reactant. The intensity of the radiation at a depth, x, into the sample is I, as can be seen in Figure 1. The decrease in the intensity of the radiation as it passes through a distance, dx, of the sample is given by

$$-dI = I(\epsilon_r + \sigma_r)[R]dx + I(\epsilon_p + \sigma_p)(R_o - [R])dx \qquad (4)$$

where ϵ is an absorption coefficient, σ a diffuse reflection coefficient, and the subscripts r and p refer to the reactant and the products, respectively.

This equation is simple the differential form of a modified Beer-Lambert relation. If α' is defined as the fraction of R_o reacted at any given time, then

$$\alpha' = (R_o - [R])/R_o . \qquad (5)$$

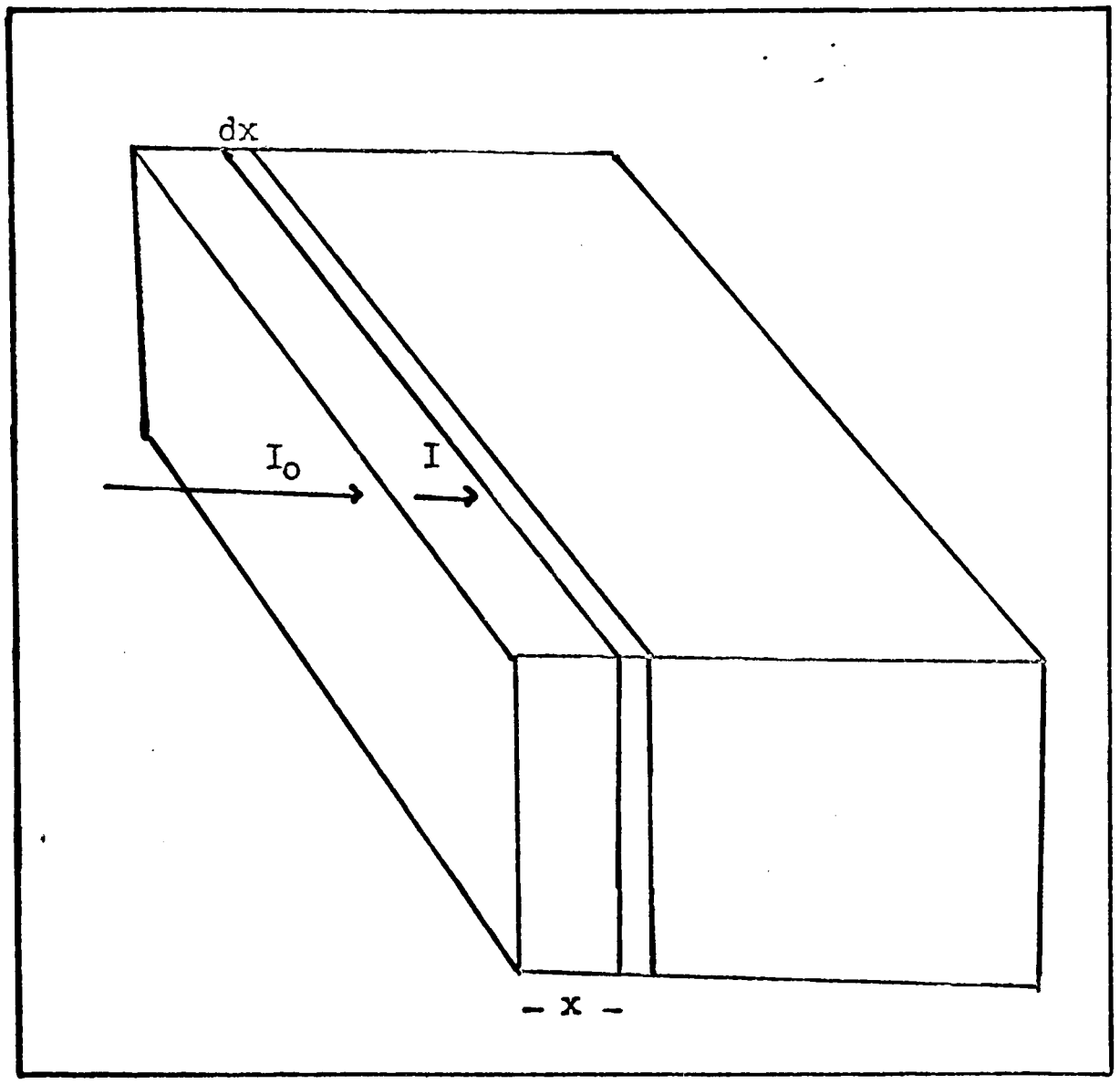

FIGURE 1

MODEL OF A POWDERED SAMPLE

Combining Equations 4 and 5 gives

$$-dI = I(\epsilon_r + \sigma_r)(1 - \alpha')R_o dx + I(\epsilon_p + \sigma_p)\alpha' R_o dx. \qquad (6)$$

Now this equation can be rearranged for integration by making use of the initial condition that $I = I_o'$ when $x = 0$ to give

$$\int_{I_o'}^{I} dI/I = \int_0^x \left[-(\epsilon_r + \sigma_r)(1 - \alpha')R_o dx - (\epsilon_p + \sigma_p)\alpha' R_o dx\right] \qquad (7)$$

and integrated to give

$$\ln(I/I_o') = -R_o(\epsilon_r + \sigma_r)x - (\epsilon_p + \sigma_p - \epsilon_r - \sigma_r)R_o \int_0^x \alpha' dx. \qquad (8)$$

The last function cannot be evaluated because the fraction reacted varies with the depth into the sample as some unknown function of x. An assumption concerning the function will be made after I has been evaluated explicitly.

Taking the exponent of both sides of Equation 8 and rearranging gives

$$I = I_o' \, e^{-R_o(\epsilon_r + \sigma_r)x - (\epsilon_p + \sigma_p - \epsilon_r - \sigma_r)R_o \int_0^x \alpha' dx}. \qquad (9)$$

If the reaction given in Equation 3 is considered to be a "bimolecular" reaction between a reactant molecule and a photon, then the following rate equation can be written:

$$-d[R]/dt = \beta[R]n \qquad (10)$$

where β is the absorption cross section for an einstein of radiation and n is the number of einsteins of photons per unit area. The number, n, is related to the intensity, I, by

$$n = I\lambda/hcN_o \qquad (11)$$

where $\underline{c}$ is the velocity of light and $\underline{N_o}$ is Avogadro's number.

Substituting Equation 10 into Equation 11 gives

$$-d[R]/dt = \beta\lambda I[R]/hcN_o. \tag{12}$$

Solving Equation 5 for $\underline{[R]}$ and substituting it and its derivative into Equation 12 gives

$$d\alpha'/dt = \beta\lambda(1 - \alpha')I/hcNo. \tag{13}$$

The substitution of Equation 9 into Equation 13 yields the equation

$$d\alpha'/dt = \left[\beta\lambda I_o'(1 - \alpha')/hcN_o\right] e^{-Ux} - V\int_0^x \alpha' dx \tag{14}$$

where $U = R_o(\epsilon_r + \sigma_r)$ and $V = R_o(\epsilon_p + \sigma_p - \epsilon_r - \sigma_r)$.

The absorption cross section is the absorption coefficient times the number of molecules of product resulting from an absorption of a photon (the quantum yield, ϕ), or

$$\beta = \phi\epsilon_r. \tag{15}$$

Substituting this equation into Equation 14 gives

$$d\alpha'/dt = \left[\lambda\phi\epsilon_r I_o'(1 - \alpha')/hcN_o\right] e^{-Ux} - V\int_0^x \alpha' dx. \tag{16}$$

Up to now the spectral or surface reflection has been neglected. The symbol, $\underline{I_o'}$, is the intensity of the radiation after surface reflection has taken place. If $\underline{q}$ is the fraction of the total initial radiation, $\underline{I_o}$, not reflected spectrally at the surface, then

$$I_o' = qI_o. \tag{17}$$

Substitution of Equation 17 into Equation 16 gives

$$d\alpha'/dt = \left[q\lambda\phi\epsilon_r I_o(1 - \alpha')/hcN_o\right] e^{-Ux} - V\int_0^x \alpha' dx. \tag{18}$$

Theoretically, Equation 18 describes the rate of the photochemical reaction of a powdered sample. However, it cannot be conveniently used as it is written. The values of q, ϵ_r, ϵ_p, σ_r, σ_p, ϕ, x, and $\alpha' = \alpha'(x)$ are not known. Several approximations must be made before this equation is in a useful form.

There is no known way to calculate the absorption coefficient of a powdered sample. However, the electronic energy levels of most compounds are independent of the state of the material. The values of the absorption coefficients obtained from measurements of the samples in aqueous solutions could therefore be used in Equation 18.

The values of the reflection coefficients can be calculated from reflectance measurements and from the values of the absorption coefficients by the use of the remission function, f (48). The remission function is related to the absorption and reflection coefficients by

$$f = \epsilon/\sigma, \tag{19}$$

and to the reflectance intensity values, r, by

$$f = r/(r - 100)^2. \tag{20}$$

The values of the reflection coefficients can therefore be determined using the remission function if the absorption coefficients are known. However, another assumption eliminates the necessity of knowing the values of the reflection coefficients. If the sample is strongly absorbing, then the radiation will penetrate to only a very small depth into the sample. If it is assumed that x is so small that

$$Ux + V\int_0^x \alpha' dx = 0 \qquad (21)$$

then Equation 18 reduces to

$$d\alpha'/dt = q\lambda\phi\epsilon_r I_o(1 - \alpha')/hcN_o. \qquad (22)$$

This approximation also eliminates the necessity of knowing the dependence of α' on the depth, x. In fact, Equation 22 also holds if the fraction of the compound reacted per unit area of the sample surface, α is substituted for α', giving

$$d\alpha/dt = q\lambda\phi\epsilon_r Io(1 - \alpha)/hcN_o. \qquad (23)$$

This substitution eliminates the necessity of knowing the volume change during the reaction.

The value of q is difficult to determine accurately. Although Fresnel's equation describes the surface reflection of a smooth solid surface, there is no equation which describes the surface reflection of a powdered sample. It has been shown, however, that the Lambert cosine law (49) which describes the diffuse reflection of a non-absorbing mat surface is approximately valid for powdered samples (50, 51). This empirical law is

$$I^* = (I_o/\pi)\cos\delta\cos\theta \qquad (24)$$

where I^* is the intensity of the radiation reflected at an angle, δ, and I_o is the intensity of the radiation striking the sample at an angle θ. In this case θ is zero since the incident radiation strikes the surface perpendicularly so that

$$I^* = \frac{I_o \cos\delta}{\pi}. \qquad (25)$$

In this investigation, the product compounds cover the immediate

surface of a sample over most of the time of a photochemical reaction and are relatively weakly absorbing over the wavelength range used. Equation 24 should therefore be approximately valid for the samples used.

The total radiation reflected diffusely, I_o', is the sum of the radiation reflected diffusely at each angle, or

$$I_o' = \sum I^* = \sum (I_o/\pi) \cos\delta. \tag{26}$$

Since the change in the angle is continuous, the summation sign can be replaced by an integral sign, or

$$I_o' = (I_o/\pi) \int_0^{\pi/2} \cos\delta \, d\delta, \tag{27}$$

which gives

$$I_o' = I_o/\pi. \tag{28}$$

The radiation striking a non-absorbing powdered surface that is not reflected diffusely is reflected spectrally. Therefore,

$$q = 1/\pi. \tag{29}$$

Substituting this value for q into Equation 23 gives

$$d\alpha/dt = \lambda\phi\epsilon_r I_o(1 - \alpha)/hcN_o\pi. \tag{30}$$

Equation 30 can be integrated to give

$$\ln(1 - \alpha) = -\lambda\phi\epsilon_r I_o t/hcN_o\pi. \tag{31}$$

Therefore a plot of $\ln(1 - \alpha)$ vs $I_o t$ yields a straight line with a slope, $-K$, given by

$$d\ln(1 - \alpha)/dI_o t = -K = -\lambda\phi\epsilon_r/hcN_o\pi. \tag{32}$$

It can be seen that the equation describing the photochemical reaction of a powdered sample (Equation 30) differs considerably

from the one describing the photochemical reaction of a fluid sample (Equation 2). This difference arises from the fact that the reactions of a powdered sample are inhomogeneous while those of a fluid sample are homogeneous and from the fact that a powdered sample reflects radiation as well as absorbs it.

Equations were also derived which describe the photochemical reactions of a solid opaque crystal and of a solid transparent crystal. Since these equations were not applicable to this investigation, they are presented in appendices. The derivation of the equation for a solid opaque crystal is given in Appendix A, page 89, and that for the solid transparent crystal is given in Appendix B, page 91.

A Derivation of Gamma

Up to now, no consideration has been made concerning the method of measuring the fraction reacted. In this investigation, reflectance measurements at 500 mμ were used to calculate the fraction reacted. Equation 38 holds for the fraction reacted of the amount of sample available to the reaction radiation. This fraction will be the same as the measured fraction reacted only if the radiation at 500 mμ penetrates the sample to the same depth as the reacting radiation. This is generally not the case. If $\underline{\alpha}^*$ is the measured fraction reacted, then

$$\alpha^* = (R_o - [R])/R_o^* \qquad (33)$$

where $\underline{R}_o^*$ is the total number of moles of reactant per unit area to

the depth that the measuring radiation penetrates. The actual fraction reacted, α, is given by

$$\alpha = (R_o - [R])/R_o \tag{34}$$

where R_o is the total number of moles of reactant per unit area available to the reacting radiation. The actual amount reacted per unit area is the same in both cases. Combining Equations 33 and 34 gives

$$\alpha^*/R_o^* = \alpha/R_o \tag{35}$$

or,

$$\alpha = \alpha^* R_o/R_o^*. \tag{36}$$

If γ is defined as follows:

$$\gamma = R_o^*/R_o \tag{37}$$

then Equation 35 can be written as

$$\alpha = \alpha^*/\gamma. \tag{38}$$

Therefore, the measured fraction reacted must be corrected by a factor of $1/\gamma$ in order to determine the actual fraction reacted.

In order to determine a theoretical expression for gamma, equations describing the reflectance of a powdered sample must be obtained. Consider a powdered sample of compound which is divided into n equal layers of thickness, d/n, where d is the mean depth. The sample is irradiated with radiation of an initial intensity of I_o. The intensity of the radiation impinging on the i^{th} layer of the sample is I_i. The amount of this radiation which is absorbed, I_{ai}, is given by Beer's law

$$I_{ai} = I_i \epsilon [R] d/n \tag{39}$$

and the amount reflected, I_{ri}, is given by

$$I_{ri} = I_i \sigma [R] d/n. \tag{40}$$

The total amount absorbed to depth d, I_a, is

$$I_a = \sum_0^n I_{ai} = \epsilon [R] d \sum_0^n I_i/n \tag{41}$$

and the total amount reflected to depth d, I_r, is

$$I_r = \sum_0^n I_{ri} = \sigma [R] d \sum_0^n I_i/n. \tag{42}$$

The value of I_n where

$$I_n = \sum_0^n I_i/n \tag{43}$$

is simply the average value of the intensity over the depth d.

If d is small, it can be assumed that

$$I_n = Io/2. \tag{44}$$

Equations 41 and 42 therefore reduce to

$$I_a = I_o \epsilon [R] d/2 \tag{45}$$

and

$$I_r = I_o \sigma [R] d/2. \tag{46}$$

Now d is given by (43)

$$d = 1/(\epsilon + \sigma)[R]. \tag{47}$$

The substitution of Equation 47 into Equations 45 and 46 gives

$$I_a = I_o \epsilon /2(\epsilon + \sigma) \tag{48}$$

and

$$I_r = I_o \sigma /2(\epsilon + \sigma). \tag{49}$$

The fraction of I_o absorbed, a, and the fraction reflected,

r, are therefore given by

$$a = \epsilon/2(\epsilon + \sigma) \tag{50}$$

and

$$r = \sigma/2(\epsilon + \sigma). \tag{51}$$

To check the validity of these equations, the value of σ for the compound, $K_3[Mn(C_2O_4)_3]\cdot 3H_2O$, at 500 m$\mu$ was calculated from the reflectance value and the absorption coefficient using Equation 51 and compared to that obtained using the more accurate remission function. The value obtained using Equation 58 was 5.2×10^4 cm^2/mole while that obtained using the remission function was 5.1×10^4 cm^2/mole. The good agreement between these values indicates that the theory presented to obtain Equations 50 and 51 is approximately valid.

Furthermore, using Equations 50 and 51, the fraction reacted as a function of the reflectance intensity values can be found to be

$$a = (\sigma_r - r\sigma_r + r\epsilon_r)/(r\sigma_p + r\epsilon_p - r\epsilon_r - r\sigma_r - \sigma_p + \sigma_r), \tag{52}$$

$$a = (27r - 2.1)/(21.8r + 1.2). \tag{53}$$

This function gives a plot of a vs r almost identical to an experimentally determined calibration curve in Figure 3 in the next chapter. This fact further supports the validity of the theory presented here.

The number of moles of compound available to the radiation, R_o, is a minimum when $\underline{a}$ is a maximum and it becomes larger as $\underline{a}$ becomes smaller. This indicates that

$$R_o \propto 1/a \tag{54}$$

or

$$R_o = R_{o_{min}}/a. \tag{55}$$

Similarly, for the measuring radiation

$$R_o^* = R_{o_{min}}/a^*. \tag{56}$$

Substitution of Equation 55 and 56 into Equation 37 for gamma gives

$$\gamma = a/a^* = (\epsilon\epsilon^* + \epsilon\sigma^*)/(\epsilon\epsilon^* + \sigma\epsilon^*). \tag{57}$$

The absorption and reflection coefficients in this equation are total. If the sample is made up of product, $\underline{R_o - [R]}$, and reactant, $\underline{[R]}$, then

$$\gamma = \frac{(\epsilon_r R + \epsilon_p(R_o - [R]))((\epsilon_r^* + \sigma_r^*)[R^*] + (\epsilon_p^* + \sigma_p^*)(R_o - [R]))}{(\epsilon_r^* R + \epsilon_p^*(R_o - [R]))((\epsilon_r + \sigma_r)[R] + (\epsilon_p + \sigma_p)(R_o - [R]))} \tag{58}$$

or

$$\gamma = \frac{(\epsilon_r + \epsilon_p a)((\epsilon_r^* + \sigma_r^*) + (\epsilon_p^* + \sigma_p^*)a^*)}{(\epsilon_r^* + \epsilon_p^* a^*)((\epsilon_r + \sigma_r) + (\epsilon_p + \sigma_p)a)} \tag{59}$$

This equation should give the correct values for the gammas.

For all of the wavelengths used in this investigation except 400 mμ

$$\epsilon_r \gg \epsilon_p$$

$$\epsilon_r^* + \sigma_r^* \gg \epsilon_p^* + \sigma_p$$

$$\epsilon_r^* \gg \epsilon_p^*$$

$$\epsilon_r + \sigma_r \gg \epsilon_p + \sigma_p. \tag{60}$$

Equation 65 therefore reduces to

$$\gamma = (\epsilon_r \epsilon_r^* + \epsilon_r \sigma_r^*)/(\epsilon_r^* \epsilon_r + \epsilon_r^* \sigma_r), \tag{61}$$

and gamma is independent of the fraction reacted for all wavelengths except 400 mμ.

The equations developed in this chapter are used to evaluate the photochemical data which are compared with the conventional thermal reaction kinetic data. These data are presented in the following chapter.

CHAPTER IV

EXPERIMENTAL METHODS AND RESULTS

Preparation and Analysis of the Compound

The kinetics of the reaction of $K_3[Mn(C_2O_4)_3] \cdot 3H_2O$ given in Equation 1 were studied in this investigation. The compound was prepared by the method of Cartledge and Ericks (41) using commercial reagent-grade chemicals. In this method, 31.5 g of oxalic acid were dissolved in 200 ml of water and heated to 75° C. Then 6.32 g of potassium carbonate were added to neutralize the oxalic acid and to supply the necessary potassium ions. After adding 150 ml of water, the solution was cooled to 0° C. From this point on, all operations were carried out in a darkened room to prevent the decomposition of the product. Upon adding stoichiometric amounts of potassium permanganate, all of the manganese in the solution was converted to the trivalent oxidation state and the solution became deep red in color. After filtering the mixture through a chilled filtering funnel, 350 ml of ethanol at 0° C were added to the filtrate. Upon allowing the solution to stand at 0° C for two hours, dark red-violet needle crystals formed. These were collected on filter paper, washed with ice-cold absolute ethanol four times, and then with anhydrous diethyl ether twice. Excess solvent evaporated from

the crystals upon standing in the dark at room temperature.

The compound, $K_3[Mn(C_2O_4)_3]\cdot 3H_2O$, was analyzed for manganese and potassium as follows: A small quantity of the compound was weighed out into a tared porcelain filtering crucible, ignited for one hour at 500° C in a muffle furnace, cooled, and weighed. This method of analysis gives a residue consisting of a mixture of K_2CO_3 and Mn_3O_4. After leaching the potassium carbonate out with water, the crucible containing only the manganese oxide was re-ignited, cooled, and weighed. The manganese content of the sample was determined from the weight of the manganese oxide, while the weight of the potassium carbonate determined the potassium content.

The water content of the compound was determined as follows: A weighed sample of the compound was placed in a porcelain boat and ignited at 500° C under a dynamic helium atmosphere. The helium and the gaseous decomposition products were permitted to pass through a weighed "U"-tube containing calcium chloride to collect the water evolved by the sample. The increase in the weight of the "U"-tube determined the water content of the sample.

The results of the analysis of the compound are given in Table I. As can seen, all of the results are within ±.3% of the theoretical values for $K_3[Mn(C_2O_4)_3]\cdot 3H_2O$, thus confirming the identity of the compound.

Photochemical Reaction Kinetics

One of the major problems that arise in the attempt to study solid-state photochemical reaction kinetics is simply the lack of a

TABLE I

ANALYSIS OF THE COMPOUND

Trial	Manganese	Potassium	Water
1.	11.5%	23.8%	10.8%
2.	11.8%	23.8%	10.4%
3.	11.3%	23.6%	10.5%
Average	11.5 ± .3%	23.7 ± .2%	10.6 ± .3%
Theoretical	11.20%	23.92%	11.02%

method of following the extent of the reaction. This problem occurs because only the immediate surface of a sample is involved in a solid-state photochemical reaction. In this investigation, mass spectrometry was attempted as a means of following the extent of the reaction by the amount of carbon dioxide evolved. This proved impossible, however, because the volume of carbon dioxide evolved was too small to detect using the apparatus and instrument available. Also, X-ray diffraction was attempted, but the X-rays penetrated through the reacted layer and did not detect it. The use of reflectance spectroscopy solved the problem.

The apparatus used in the photochemical kinetic studies is illustrated in Figure 2. Samples of the compound were contained in a circular aluminum sample holder. The sample container was placed in a vertical position and the sample was irradiated with monochromatic radiation from a Bausch and Lomb monochromator with a mercury-vapor radiation source. The intensity of the radiation was controlled by adjusting the slit width and measured with a Ysi-Kettering Model 65 radiometer. A Timit timer measured the length of time of irradiation. Samples were irradiated with radiation of a specific intensity and wavelength for periods of time from 1-15 min in duration. The sample holder was then removed and the visible reflectance spectra of the samples were obtained by the use of a Beckman Model DK-2 A spectroreflectometer after each short period of irradiation.

The spectra illustrated in Figure 3 were obtained from a sample irradiated with radiation of an intensity of 2.6×10^{4} erg/cm^2 sec and

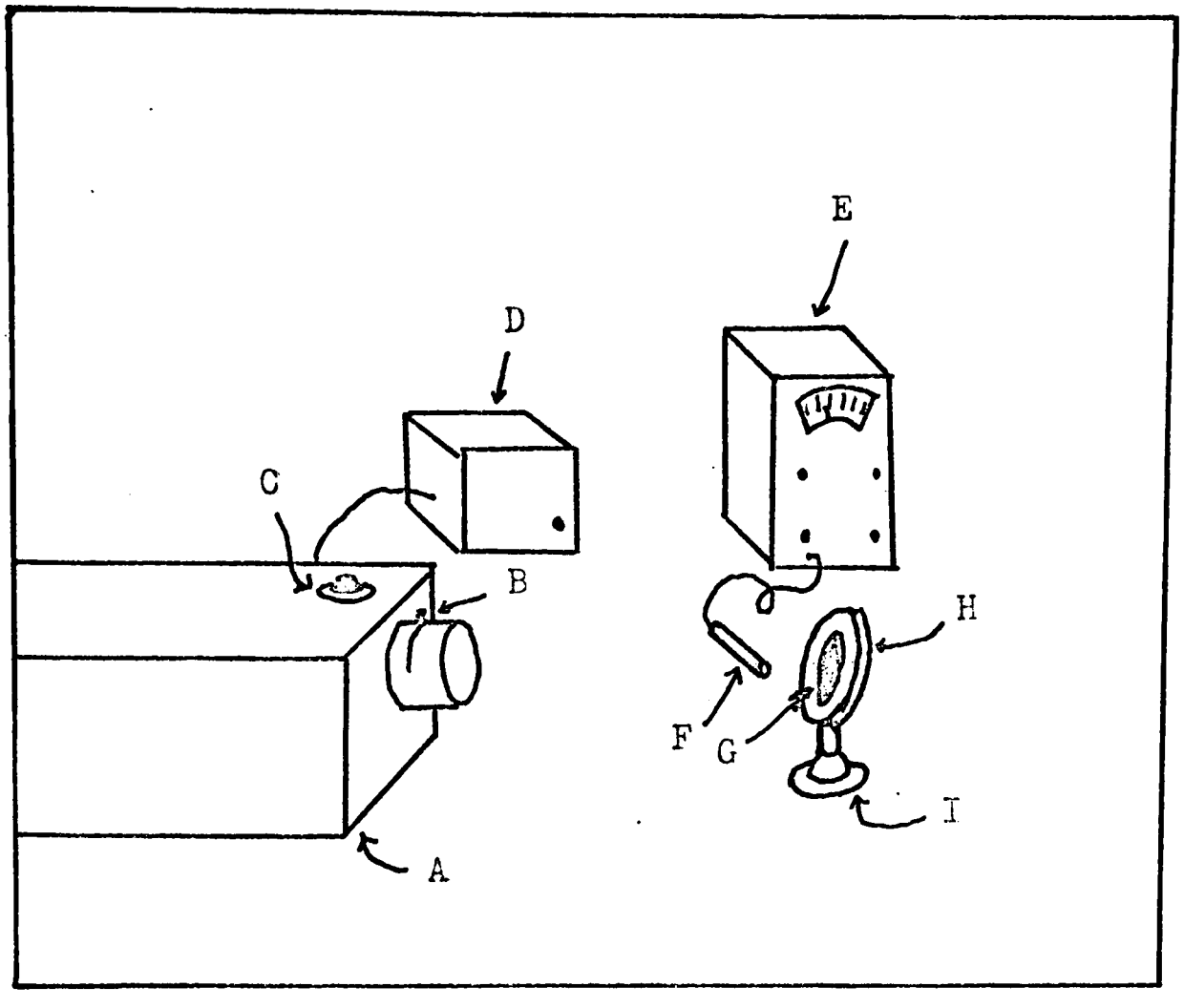

FIGURE 2

APPARATUS

A. Monochrometer
B. Slit Width Adjuster
C. Wavelength Control
D. Mercury Vapor Light Source
E. Radiometer
F. Detector
G. Sample
H. Sample Holder
I. Sample Holder Stand

FIGURE 3. Sample Reflectance Spectra (λ= 250 mμ I_o = 2.6 x 10^4 erg/cm^2 sec)

Spectrum of pure $K_3[Mn(C_2O_4)_3] \cdot 3H_2O$ ——————

Spectrum after 15 min irradiation —•—•—•—

Spectrum after 30 min irradiation —— —— —

Spectrum after 60 min irradiation - - - - - - - - -

Spectrum after 90 min irradiation —— . —— . —

Spectrum after 120 min irradiation —— . . —— . . —

Spectrum of product compounds —|—|—|—

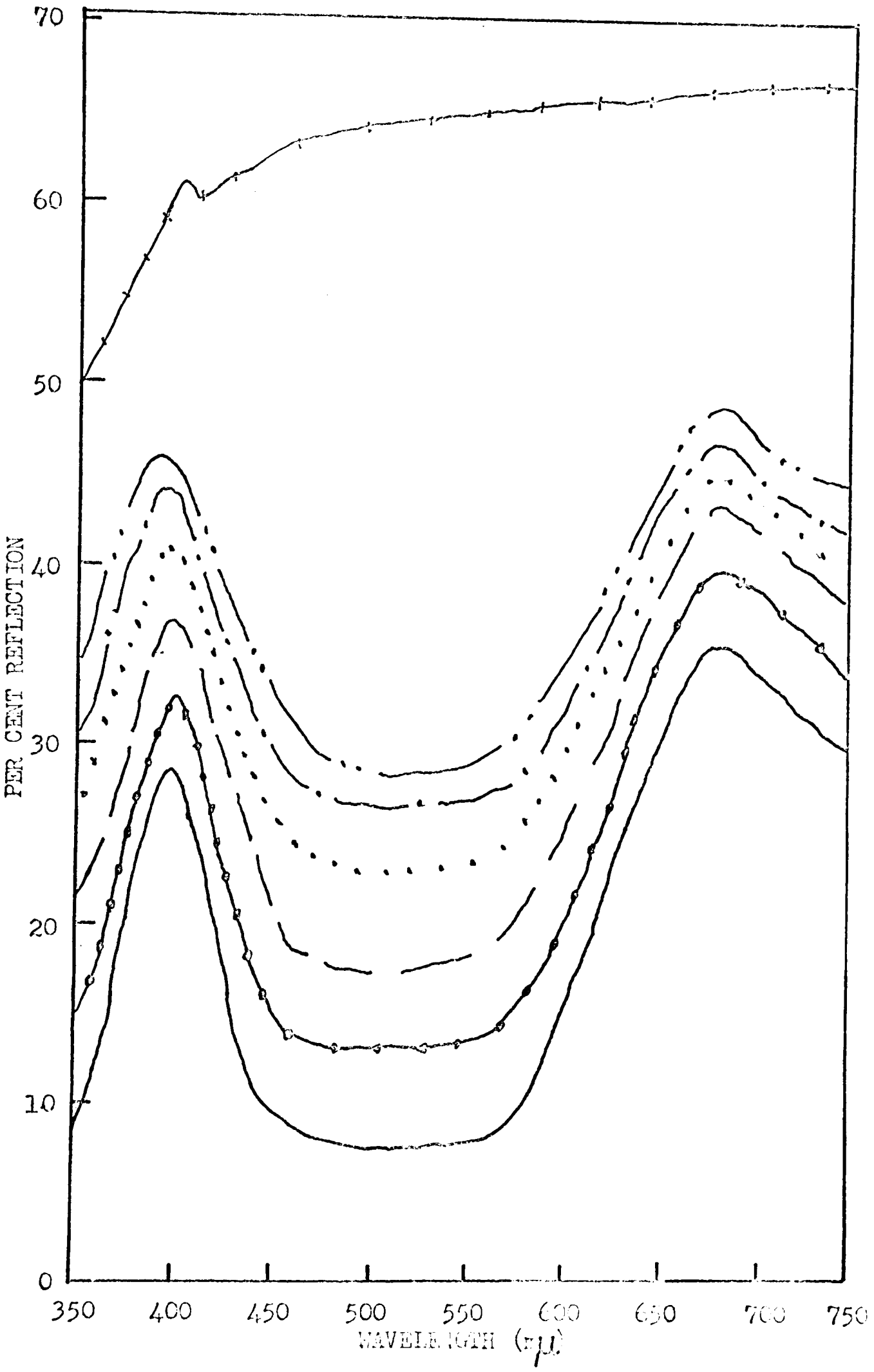
70
60
50
40
30
20
10
0
PER CENT REFLECTION
350
400
450
500
550
600
650
700
750
WAVELENGTH (mμ)

a wavelength of 250 mμ. As can be seen, there is a change in the reflectance intensity of the spectra over the entire wavelength range from 350-750 mμ as the sample reacts. However, since the largest change in the reflectance intensity occurred at about 500 mμ, this wavelength was chosen for the purpose of measuring the extent of the reaction in order to minimize the error.

Reflectance spectroscopy is a relatively new technique and no quantitatative expressions relating fractions reacted to reflectance intensities have been developed. However, since reflectance intensities depend upon the composition of the sample, it must be possible to calculate fractions reacted from them. Absolute reflectance intensities depend upon the sample particle size and the degree of packing of the sample. In a kinetic investigation, however, it is not necessary to know the absolute reflectance intensities, but only the relative intensities of the reflectance spectra of a sample during a kinetic run. Since one sample is used throughout each kinetic run, the sample particle size and degree of packing are constant for each run. Furthermore, in this investigation, in order to minimize reflectance intensity differences of different samples, care was taken to grind each sample for the same length of time and to pack each sample in the sample holder in the same manner. The result of these precautions was a probable error of ±3% for the reflectance intensities of 35 samples of the pure reactant compound at 500 mμ.

It therefore appears possible to use reflectance intensity measurements to calculate fractions reacted for the purpose of this

investigation. Methods for calculating sample compositions from reflectance intensities have previously been reported (42, 43). However, since it was not known which of these methods may be suitable for the compound used in this investigation, a calibration curve was prepared for the purpose of determining fractions reacted from reflectance intensity values. Known quantities of $K_3[Mn(C_2O_4)_3]\cdot 3H_2O$ and its reaction products prepared by pyrolysis of the reactant according to Equation 1 were intimately mixed and their reflectance spectra obtained. Reflectance spectra were obtained for five different mixtures of each composition. From this data, which is given in Table II, a calibration curve was made from which the fraction reacted could be found if the reflectance intensity at 500 mμ was known. This calibration curve is given in Figure 4.

Thermal Reaction Kinetics

The thermal reaction kinetics for the decomposition of the compound, $K_3[Mn(C_2O_4)_3]\cdot 3H_2O$, were studied using an instrument specially built in this laboratory which simultaneously measured the weight loss and the magnetic susceptibility of the sample (44). The weight loss of the sample, however, could not be used for a kinetic investigation of the oxidation-reduction reaction because, unlike the photochemical reaction, the water is evolved in a different step in the thermal reaction. However, this step overlaps the oxidation-reduction step and the weight loss of only the carbon dioxide cannot be followed. In the high-spin configuration of d^2sp^3 octahedral manganese(III) compounds, such as potassium

TABLE II

CALIBRATION CURVE DATA

Trial	Mole Fraction of Product	Per Cent Reflection	Mole Fraction of Product	Per Cent Reflection
1	.224	13.0	.312	17.1
2		13.1		16.3
3		14.2		16.0
4		13.2		15.8
5		12.3		16.2
Average		13.2 ± .8		16.3 ± .6
1	.541	25.0	.783	42.1
2		23.1		42.0
3		25.5		41.6
4		24.5		41.2
5		26.6		42.8
Average		24.9 ± 1.3		41.9 ± .7
1	.650	33.0	.883	57.0
2		31.4		55.3
3		30.2		54.2
4		32.1		56.4
5		31.4		55.8
Average		31.6 ± 1.2		55.3 ± 1.3
1	.961	61.5	1.000	65.0
2		61.8		63.4
3		61.2		66.1
4		60.0		65.2
5		63.1		65.1
Average		61.5 ± 1.2		64.9 ± 1.1

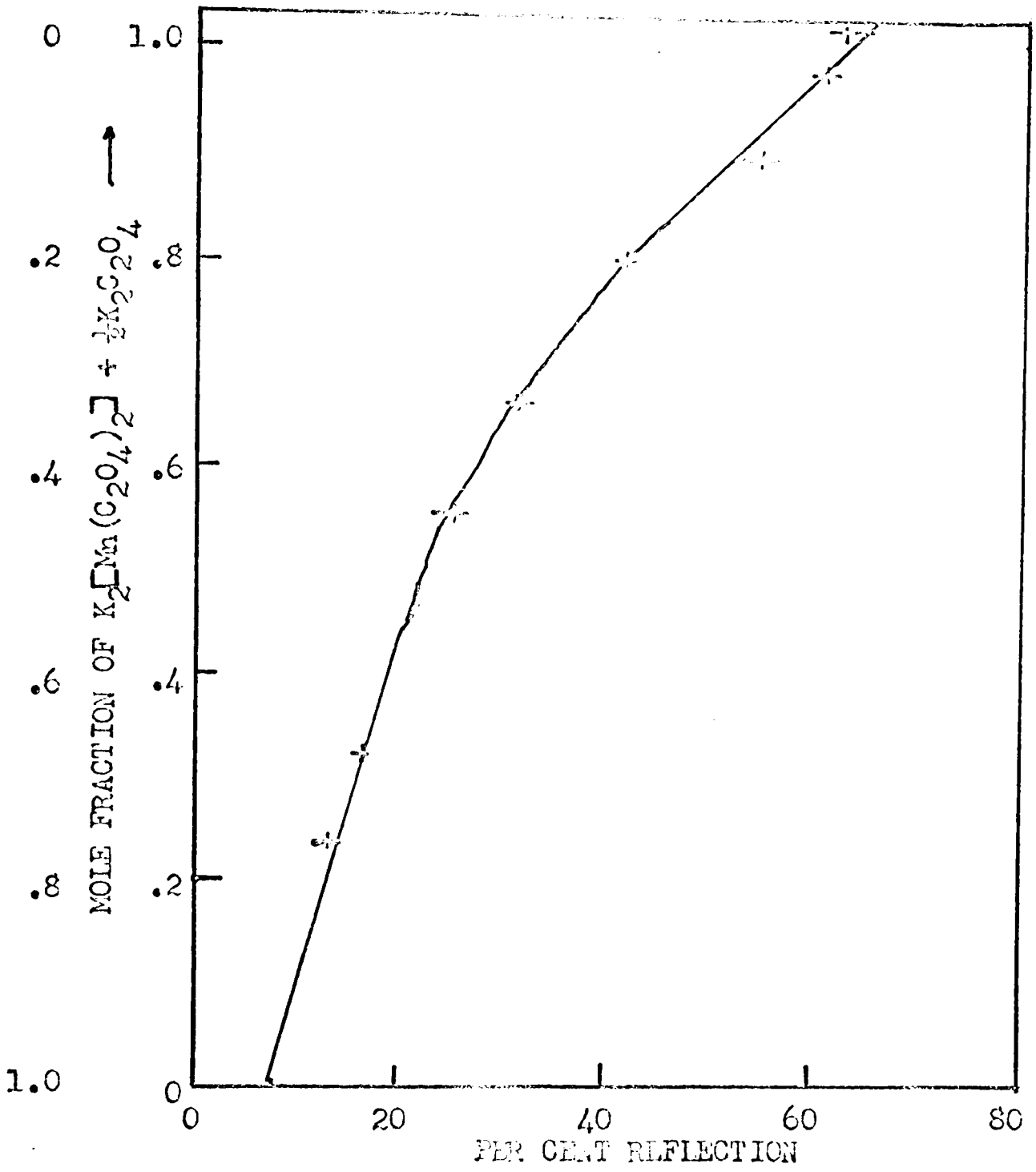

FIGURE 4

CALIBRATION CURVE

tris(oxalato)manganate(III) 3-hydrate, the manganese contains four unpaired electrons. Manganese(II) in compounds such as the products of the reaction given in Equation 1, has five unpaired electrons. From the spin only formula (45),

$$\mu = \left[n(n + 2)\right]^{\frac{1}{2}} \qquad (62)$$

where μ is the magnetic moment and n is the number of unpaired electrons, which applies very well to both manganese(III) and manganese(II) compounds, the magnetic moments are 4.90 and 5.92 B. M., respectively. This difference allows the extent of the reaction to be determined from magnetic susceptibility measurements.

The instrument used in this investigation made use of the Faraday method of measuring magnetic susceptibilities. It consisted of an Ainsworth Model RV-AV-2K semi-micro automatic recording balance equipped with a two-pen strip-chart recorder; a 4-inch Alpha Instruments aluminum-foil wound electromagnet fitted with Heyden type pole pieces; a 0-10 amp regulated-magnet power supply; a Pyrex glass tube furnace chamber, non-inductively wound with Nichrome resistance wire, and insulated with several layers of asbestos paper; a furnace temperature programmer consisting of a variable transformer; and a magnet platform which could be raised or lowered by means of a 2-ton capacity hydraulic piston and pump assembly. The sample was contained in a small Pyrex glass bucket attached to the left balance pan by a gold wire. A Chromel-Alumel thermocouple placed in the furnace at a position just below the sample bucket detected the furnace temperature. A sample of from 15-25 mg was placed in the sample container. The furnace assembly was positioned about

the sample. The magnet power supply was adjusted to maintain a maximum magnetic field of 4000 gauss. By manual operation, the hydraulic pump was used to raise the magnet about the furnace, so that the sample passed through the inhomogeneous magnetic field. Meanwhile, the apparent mass change of the sample was being recorded. After adjusting the temperature programmer to maintain a given constant temperature within $\pm.5^{o}$ C, the magnet was raised and then lowered every few minutes to obtain the magnetic susceptibility. Isothermal kinetic runs, from which the kinetic data were obtained, were made at 75^{o}, 80^{o}, and 85^{o} C.

In the Faraday method, the apparent mass change as a sample passes through an inhomogeneous magnetic field is related to the magnetic susceptibility by (46)

$$g \Delta m = \chi m H \, dH/dx \qquad (63)$$

where g is the gravitational constant, Δm the apparent mass change, χ the mass magnetic susceptibility, m the mass of the sample, H the magnetic field strength, and dH/dx the magnetic field gradient. By Equation 63, when $H \, dH/dx$ is a maximum then the apparent mass change, Δm, is also a maximum. Thus, if the apparent mass change of a sample of known magnetic susceptibility is compared with that of one with an unknown magnetic susceptibility, $H \, dH/dx$ is replaced by $(H \, dH/dx)_{max}$, and the two resulting equations combined, then the following is obtained:

$$\chi_u = \chi_s (\Delta m_u - \Delta m_c)/(\Delta m_s - \Delta m_c) \, m_s/m_u \qquad (64)$$

where u, s, and c refer to the unknown sample, the standard sample, and the sample container, respectively. The magnetic susceptibility

of a sample can therefore be determined from the maximum apparent mass change by the use of a standard compound of known magnetic susceptibility. In this investigation, $(NH_4)_2Fe(SO_4)_2 \cdot 6H_2O$ with a magnetic susceptibility of 32.3×10^{-6} c. g. s. units, was used as the standard compound.

The magnetic moment of the sample was calculated from the magnetic susceptibility by the use of the equation

$$\mu = 2.84(\chi_m T)^{\frac{1}{2}} \qquad (65)$$

where T is the absolute temperature, χ_m the corrected molar magnetic susceptibility, and μ the magnetic moment.

The fraction of the compound reacted, α, at any given time of reaction was calculated using the equation below which has previously been derived (44):

$$\alpha = \frac{(\Delta_m - \Delta_{m_o})/(\Delta_{m_s} - \Delta_{m_c})\ (T\ 8.07\ m_s \chi_s - \mu_p^2 N)}{\mu_r^2 - \mu_p^2} \qquad (66)$$

where N is the total number of moles of compound and r and p refer to the reactant and the product compounds, respectively.

To determine the effect of the evolution of the water of hydration on the oxidation-reduction reaction, runs were made at the low temperatures of 50°, 57°, and 59° C. At these low temperatures, the water is slowly evolved but the oxidation-reduction reaction should not occur if the evolution of the water does not initiate it. These runs were carried out in a constant temperature reaction vessel and the extent of the reaction was followed by weight loss.

Calculation of Absorption Coefficients

No way could be found to measure the absorption coefficients

of $K_3[Mn(C_2O_4)_3] \cdot 3H_2O$ in the solid state. They were therefore measured with the compound in aqueous solutions. Since the compound reacts in water, after dissolving weighed samples, the absorbances of the solutions were determined by the use of an Hitachi Model 139 spectrophotometer every few seconds for several minutes. The absorbance values were determined by extrapolating to zero time. From the absorbance values, the absorption coefficients were calculated using Beer's law:

$$A = \epsilon bc \tag{67}$$

where A is the molar absorbance, ϵ the molar absorption coefficient, b the length of the cell in cm, and c the concentration in mole/cm^3. Absorption coefficients were calculated at wavelengths of 275, 300, 350, 375, and 400 mμ. The values are given in Table III.

Treatment of the Data

The data in this investigation were analyzed according to the method of least squares and the probable errors were calculated. Measurements deviating more than four times the probable error from the least square values were rejected.

The Calculation of Gamma

Equation 61 was used to calculate the values of gamma for each wavelength used in this investigation except 400 mμ. It was assumed that an average value of gamma at 400 mμ during a reaction would give approximately correct alpha values. Therefore values of gamma were obtained using Equation 59 for the fraction reacted equal to zero

TABLE III

ABSORPTION COEFFICIENTS

Wavelength (mμ)	Absorption Coefficient (cm^2/mole)
250	5.0×10^7
275	8.1×10^6
300	3.2×10^6
325	9.0×10^5
350	2.5×10^5
375	6.0×10^4
400	5.1×10^4

and for the fraction reacted equal to one. These two values were averaged and the resulting value was assumed to be approximately the correct value of gamma at 400 mμ. The values of the absorption coefficients for the reacting radiation used in these calculations were taken from Table III. The value of the absorption coefficient for the measuring radiation of 500 mμ has previously been determined to be 3.08×10^5 cm^2/mole (52). The values of the reflection coefficients were calculated from the reflectance values and the values of the absorption coefficients by the use of Equation 51. The calculated values of gamma are given in Table IV. These values were used to correct the measured values of the fraction reacted according to Equation 38.

As further proof that Equation 61 gives correct values of the gammas, an iteration method was used to calculate the values of the gammas from the photochemical data. These values are also given in Table IV for comparison. The good agreement between these values supports the validity of the theoretical derivation of the expression for gamma.

Photochemical Reaction Kinetic Results

In order to test the validity of Equation 30 which describes the rate of the photochemical reaction of a powdered sample, photochemical data were obtained for the reaction of potassium tris(oxalato)-manganate(III) 3-hydrate. This deep red-violet compound reacts upon irradiation with radiation of wavelength from 250-400 mμ according to Equation 1 to give white colored products.

TABLE IV

THE VALUES OF GAMMA

Wavelength	Gamma	Gamma (Iterated)
250	.720	.70
275	.810	.79
300	.854	.84
325	.885	.90
350	1.012	1.00
375	1.195	1.22
400	1.252	1.23

According to Equation 31, if the theory is correct, a plot of $\ln(1 - \alpha)$ vs $I_o t$ should yield a straight line with a slope of $-\lambda\phi\epsilon_r/hcN_o\pi$. Plots were obtained at wavelengths of 400, 375, 350, 325, 300, 275, and 250 mμ. All of these curves were straight lines, just as Equation 31 predicts. The data used to make these plots are given in Appendix D, page 106. For convenience, the plot for the wavelength of 350 mμ is given in Figure 5. Since all of the other plots are similar, they are given in Appendix C, page 93.

If Equation 31 is correct, then the rate constants, K, obtained from the slopes of the curves in Figures 5 and 13-18 should be given by Equation 32. Upon rearranging Equation 32, the quantum yield is given by

$$\phi = KhcN_o\pi/\lambda\epsilon_r. \qquad (68)$$

The values of K for each wavelength are given in Table V. Using these values of K and the values of ϵ_r from Table III, Equation 68 was used to calculate the value of the quantum yield for each wavelength. These values are also given in Table V. The average value of the quantum yield was found to be

$$\phi = 1.71 \pm .32. \qquad (69)$$

However, as can be seen from the quantum yield values in Table V, the values at 300 and 275 mμ are lower than those at the other four wavelengths. This, however, is expected. According to previous spectral studies (53), a strong absorption band maximum of bound oxalate ions appears at about 250 mμ. Parts of this band can be seen in the ultraviolet reflectance spectra in Figure 6 where both the

FIGURE 5. Rate Plot (350 mμ).

I_o (erg/cm^2 sec)	
3.0×10^4	O
4.2×10^4	O
5.6×10^4	◐
7.2×10^4	⊖
1.1×10^5	⊙

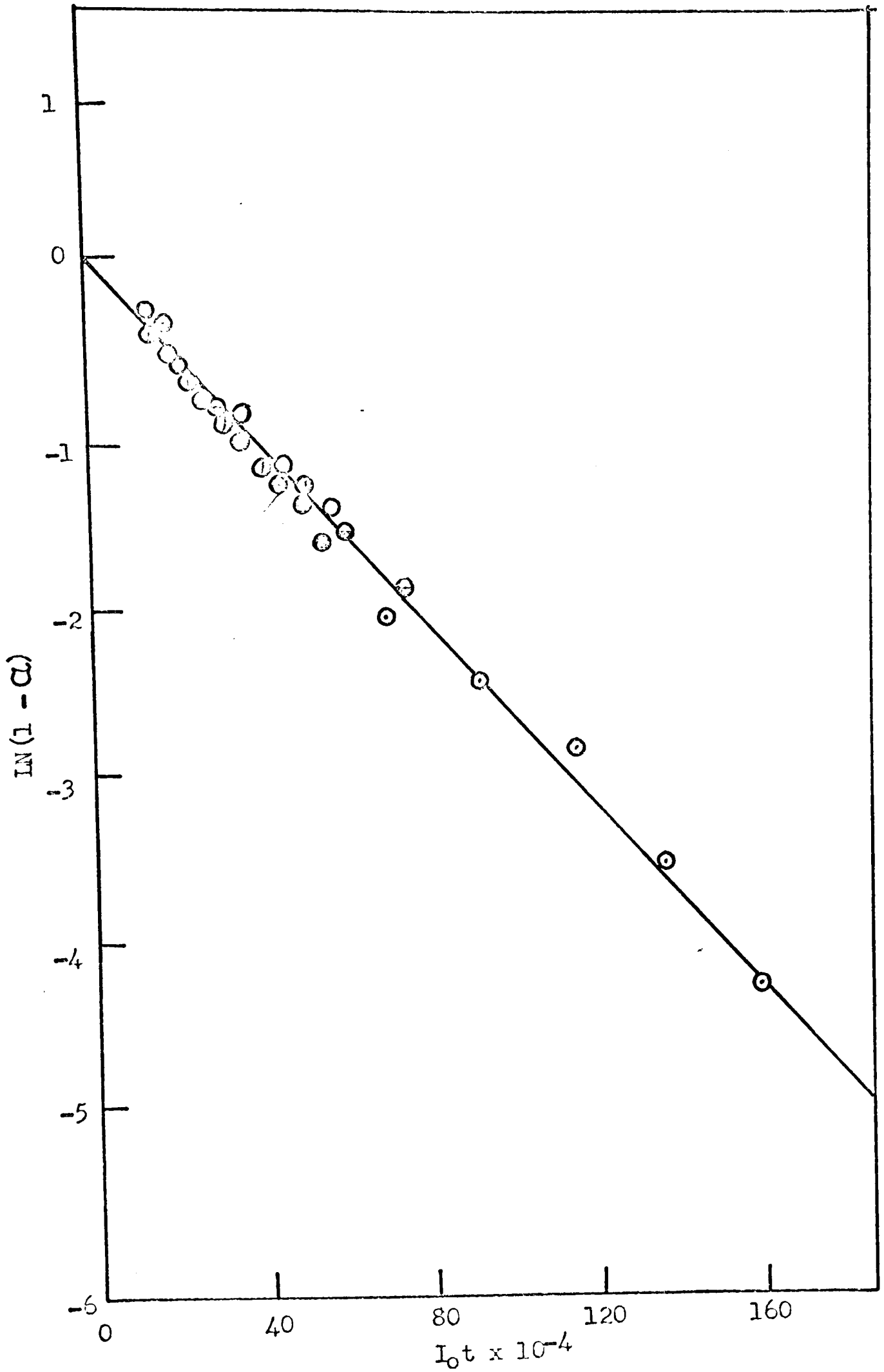
1
0
-1
-2
-3
-4
-5
-6
LN(1 - α)
0
40
80
120
160
$I_o t \times 10^{-4}$

TABLE V

PHOTOCHEMICAL RATE CONSTANTS

Wavelength (mμ)	Rate Constant (1/sec)	
275	$7.01 \pm .20 \times 10^{-7}$	1.12
300	$2.92 \pm .15 \times 10^{-7}$	1.16
325	$1.78 \pm .11 \times 10^{-7}$	2.22
350	$4.63 \pm .14 \times 10^{-8}$	1.99
375	$1.01 \pm .06 \times 10^{-8}$	1.69
400	$1.15 \pm .07 \times 10^{-7}$	2.08

FIGURE 6. Ultraviolet Reflectance Spectra.

Reactant ——————————

Products — — — — — —

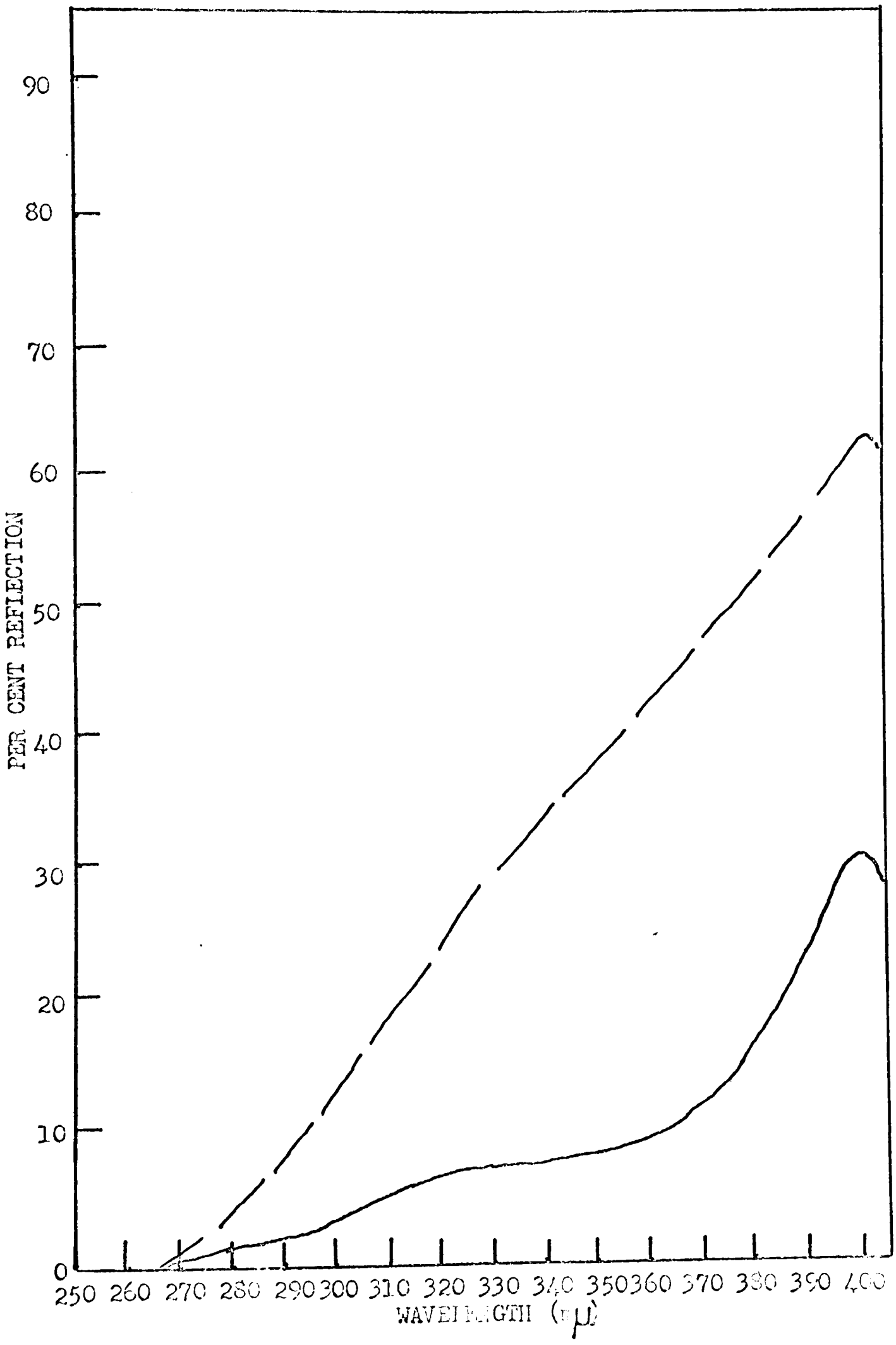
PER CENT REFLECTION
90
80
70
60
50
40
30
20
10
0
250 260 270 280 290 300 310 320 330 340 350 360 370 380 390 400
WAVELENGTH (mμ)

reactant and the products absorb strongly over the wavelength range of 300-250 mμ. The charge-transfer band of the reactant can be seen as a shoulder on the bound oxalate-ion absorption band over the wavelength range in which reaction occurs. Thus at 300 and 275 mμ absorption of some of the radiation by the bound oxalate ions which does not result in reaction causes the quantum yield to be less than at the other wavelengths. Therefore, a more accurate value of the quantum yield can be obtained by averaging all of the quantum yield values except those at 300 and 275 mμ. This value is

$$\phi = 1.99 \pm .17. \tag{70}$$

A quantum yield of two for the reaction given in Equation 1 would be expected on the basis of the stoichiometry. Since one oxalate ion must reduce two metal ions, it may be expected that the absorption of one photon may cause two molecules to react.

On the basis of the results presented in this section, the theory presented in the previous chapter appears to be valid for the photochemical reaction of powdered potassium tris(oxalato)-manganate(III) 3-hydrate.

The Dependence of the Rate on the Wavelength

Since, except for λ itself, the absorption coefficient is the only number in the expression for the photochemical rate constant which depends on the wavelength of the radiation, the values of the absorption coefficients were plotted with the reciprocal of the wavelengths. This plot is given in Figure 7. The value of the absorption coefficient at 250 mμ was calculated using Equation

FIGURE 7. Plot of Absorption Coefficients With Wave Numbers

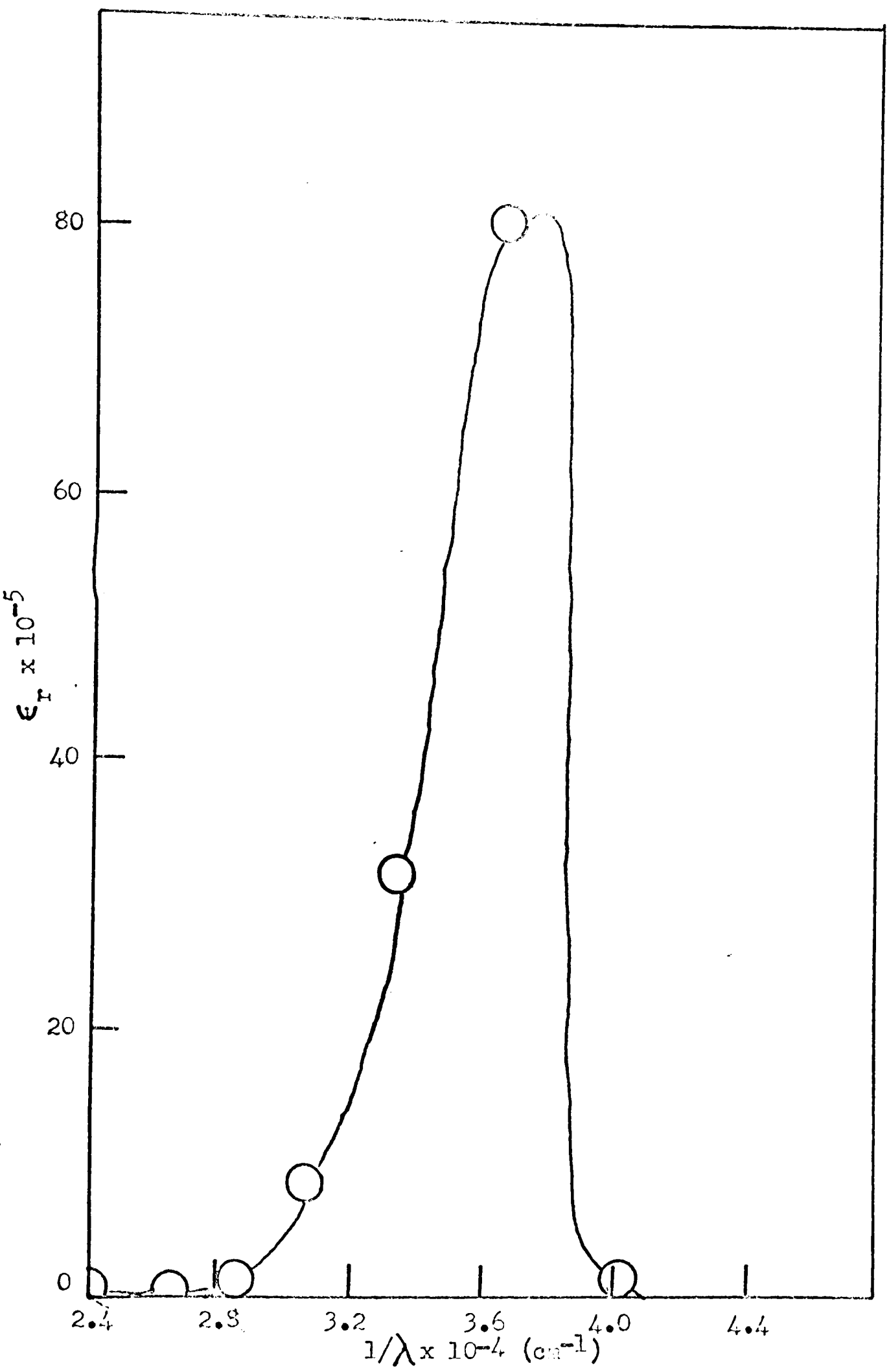
80
60
40
20
0
ε^{max} x 10^{-5}
2.4
2.8
3.2
3.6
4.0
4.4
$1/\lambda$ x 10^{-4} (cm^{-1})

68. The strong absorption band maximum of the bound oxalate ions at about 250 mμ which was mentioned previously causes the actual value of the absorption coefficient at this wavelength to be large, while the calculated value for the charge transfer band is small.

The values of the absorption coefficients appear to rise exponentially from 400 mμ to about 270 mμ beyond which there is a sharp drop. A plot of the natural logarithms of the absorption coefficients with the reciprocal of the wavelenths was made. The values used are given in Table VI and the plot is given in Figure 8. As can be seen, this plot is a straight line. Therefore,

$$d\ln \epsilon_r / d(1/\lambda) = B \tag{71}$$

or,

$$\ln \epsilon_r = B/\lambda + C \tag{72}$$

and

$$\epsilon_r = e^{B/\lambda}\ e^{C}, \tag{73}$$

where B and C are constants. Substitution of this equation into Equation 38 gives

$$d\alpha/dt = \frac{I_o \lambda \phi (1-\alpha)\ e^{B/\lambda}\ e^{C}}{hcN_o \pi}. \tag{74}$$

This equation gives the dependence of the rate of the photochemical reaction on the wavelength of the radiation. The exponential dependence probably arises from a Boltzmann distribution factor.

Since most of the molecules are in their ground vibrational energy levels at room temperature, the maximum rate of a photochemical reaction should occur when radiation with a wavelength corresponding to the difference between the ground vibrational level of the lower

TABLE VI

THE NATURAL LOGS OF THE ABSORPTION COEFFICIENTS

Wavelength ($m\mu$)	1/Wavelength (cm^{-1})	Ln ϵ_r
275	3.64×10^4	15.87
300	3.33×10^4	14.95
325	3.07×10^4	13.68
350	2.86×10^4	12.42
375	2.67×10^4	11.64
400	2.50×10^4	10.81

FIGURE 8. Plot of the Natural Log of the Absorption Coefficient With the Wave Number

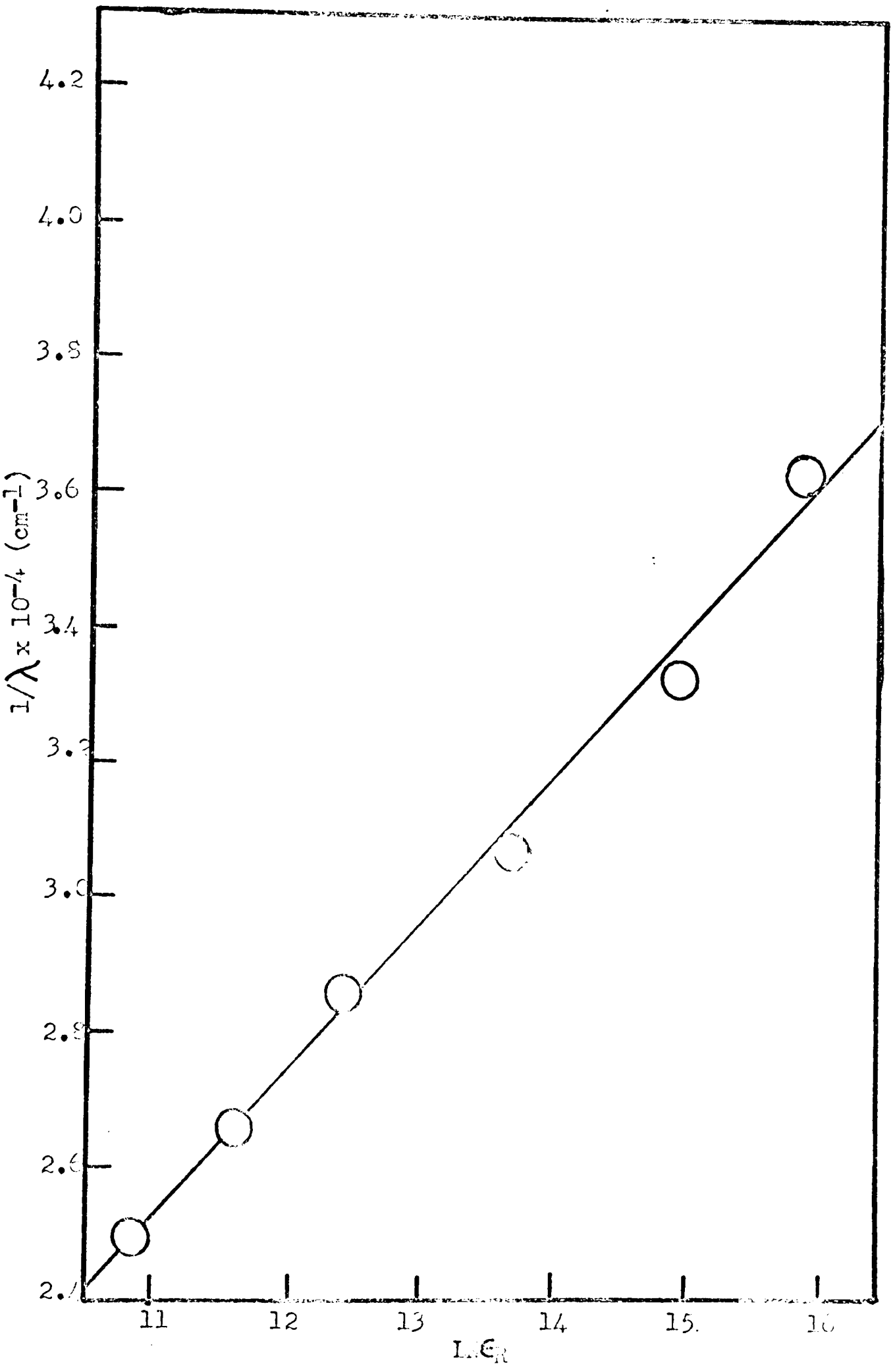
4.2
4.0
3.8
3.6
3.4
3.2
3.0
2.8
2.6
2.4
$1/\lambda \times 10^{-4}$ (cm^{-1})
11
12
13
14
15.
16
$\log_{10} R$

electronic energy state and the excited electronic energy state is used. From Figure 7, it can be seen that the maximum reaction rate occurs using radiation between 260-280 mμ. This gives an energy value, E, of

$$E = 106 \pm 4 \text{ Kcal/mole.} \tag{75}$$

The thermal activation energy will later be compared to the photochemical energy. It can be seen from Figure 7 that energies less than E will cause the reaction to occur. Perhaps the best number for comparison with the thermal activation energy would be the energy corresponding to the average rate of the reaction between 250-400 mμ. This number was determined by averaging the values of ϵ_r over the curve in Figure 7 and taking the wavelength at which the average value of ϵ_r corresponded as a measure of the average excitation energy, E_p^*. This energy was found to be

$$E_p^* = 100 \pm 4 \text{ Kcal/mole.} \tag{76}$$

Thermal Reaction Kinetics

The compound, potassium tris(oxalato)manganate(III) 3-hydrate, reacts according to Equation 1 very rapidly over a narrow temperature range. Table VII gives the values of the fraction reacted at various times obtained during isothermal kinetic runs taken at 75°, 80°, and 85° C.

To find the reaction order, the rate equation was assumed to have the form given below:

$$dP/dt = K M^n \tag{77}$$

where M is the concentration of the reactant, P is the concentration

TABLE VII

THERMAL KINETIC DATA

Time (sec)	Fraction Reacted	$1/M \times 10^{-4}$
Temperature = 75° C	$1/T = 2.875 \times 10^{3}$	K = 18.8 lnK = 2.92
198	.13	2.22
390	.29	2.71
576	.37	3.06
810	.48	3.71
1068	.54	4.17
Temperature = 80° C	$1/T = 2.835 \times 10^{3}$	K = 136.5 lnK = 4.92
162	.22	3.28
264	.53	5.45
438	.65	7.32
Temperature = 85° C	$1/T = 2.795 \times 10^{3}$	K = 777.0 lnK = 6.71
111	.40	3.38
180	.77	8.54
288	.85	13.50

of the product, K is the rate constant, and n is the reaction order. If the logarithm of both sides of Equation 77 is taken, the following is obtained:

$$\log(dP/dt) = \log K + n\log M. \tag{78}$$

Differentiation with respect to logM gives

$$d\log(dP/dt)/d\log M = n. \tag{79}$$

The slope of a plot of log(dP/dt) vs logM is therefore the order of the reaction.

Figure 9 illustrates a plot of the fraction reacted with time for the reaction at 75° C. From this curve, the data in Table VIII was obtained. From these data the plot in Figure 10 was made to determine the reaction order. The slope of this line was found to be two. Therefore, the rate equation is

$$-dM/dt = dP/dt = KM^2 \tag{80}$$

or

$$d(1/M)/dt = K. \tag{81}$$

Figure 11 illustrates plots of 1/M vs t for runs obtained at temperatures of 75°, 80°, and 85° C. In these plots, M was not the number of moles per unit volume, but was the total number of moles of reactant. Since many solid compounds undergo volume changes during reaction, the concentration cannot be expressed in units of moles per unit volume. The values of 1/M used to make these plots are also given in Table VII. The slopes of the plots in Figure 11 were obtained as the values of the rate constants and are also given in Table VII.

The Arrhenius equation is

FIGURE 9. Thermal Rate Plot

Temperature = 75° C.

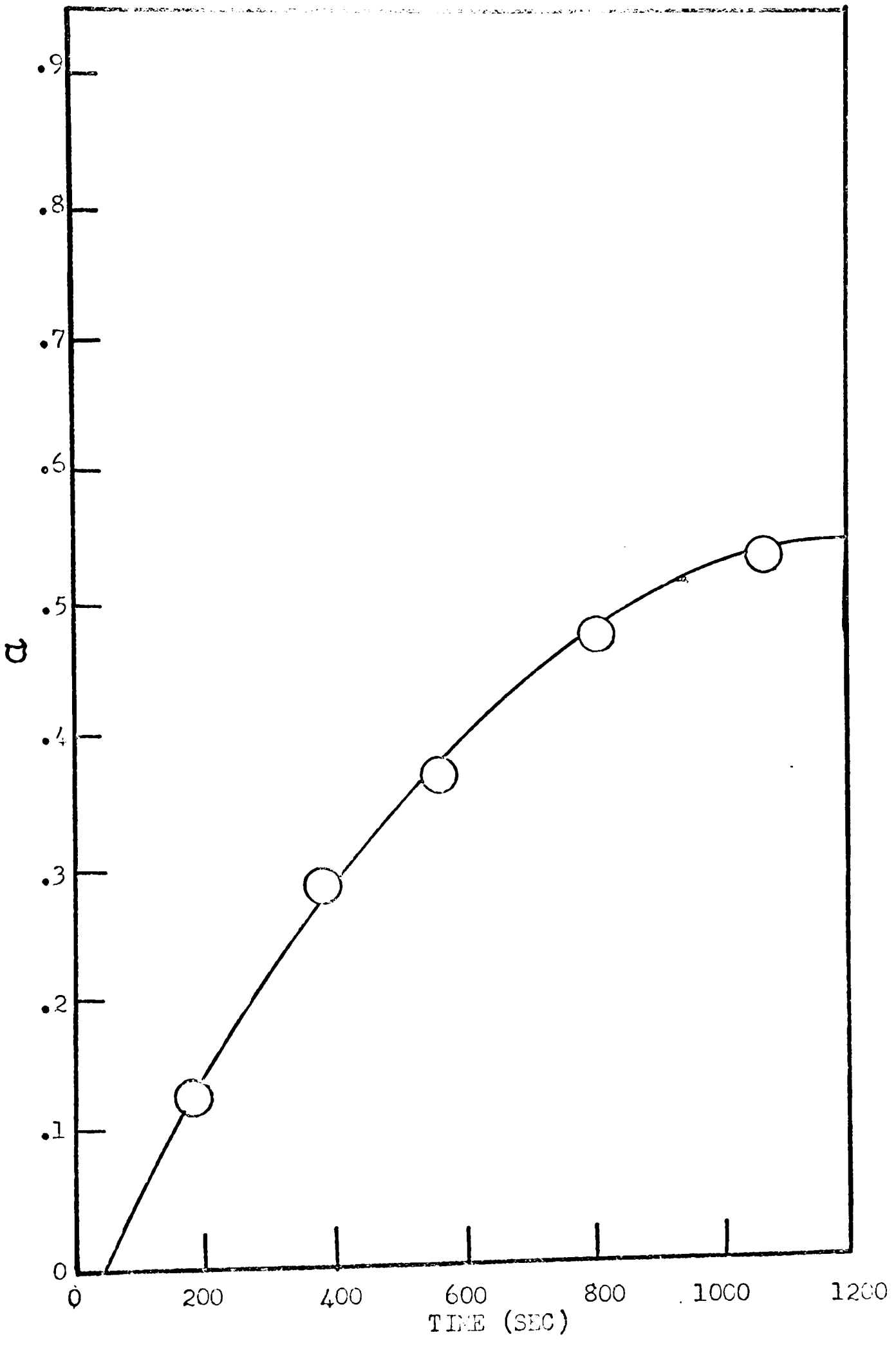
.9
.8
.7
.6
.5
.4
.3
.2
.1
0
α
0
200
400
600
800
1000
1200
TIME (SEC)

TABLE VIII

DATA OBTAINED TO FIND THE REACTION ORDER

Log(rate)	Log($\bar{M}$)
.902	1.914
.845	1.872
.699	1.796
.544	1.728
.477	1.702

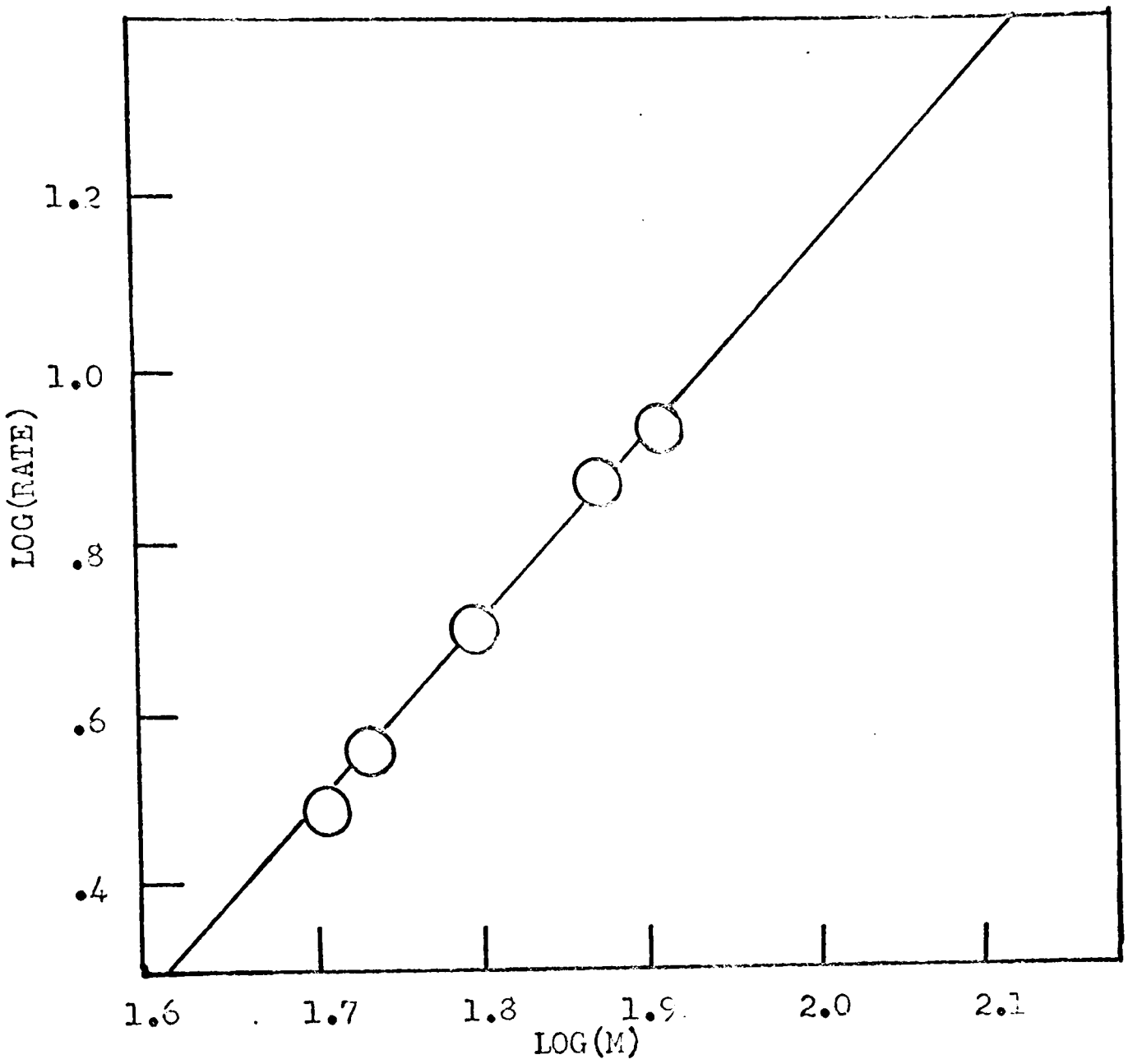

FIGURE 10

THE ORDER OF THE THERMAL REACTION

FIGURE 11. Second Order Rate Plots

Temperature

75° C ○

80° C ◑

85° C ●

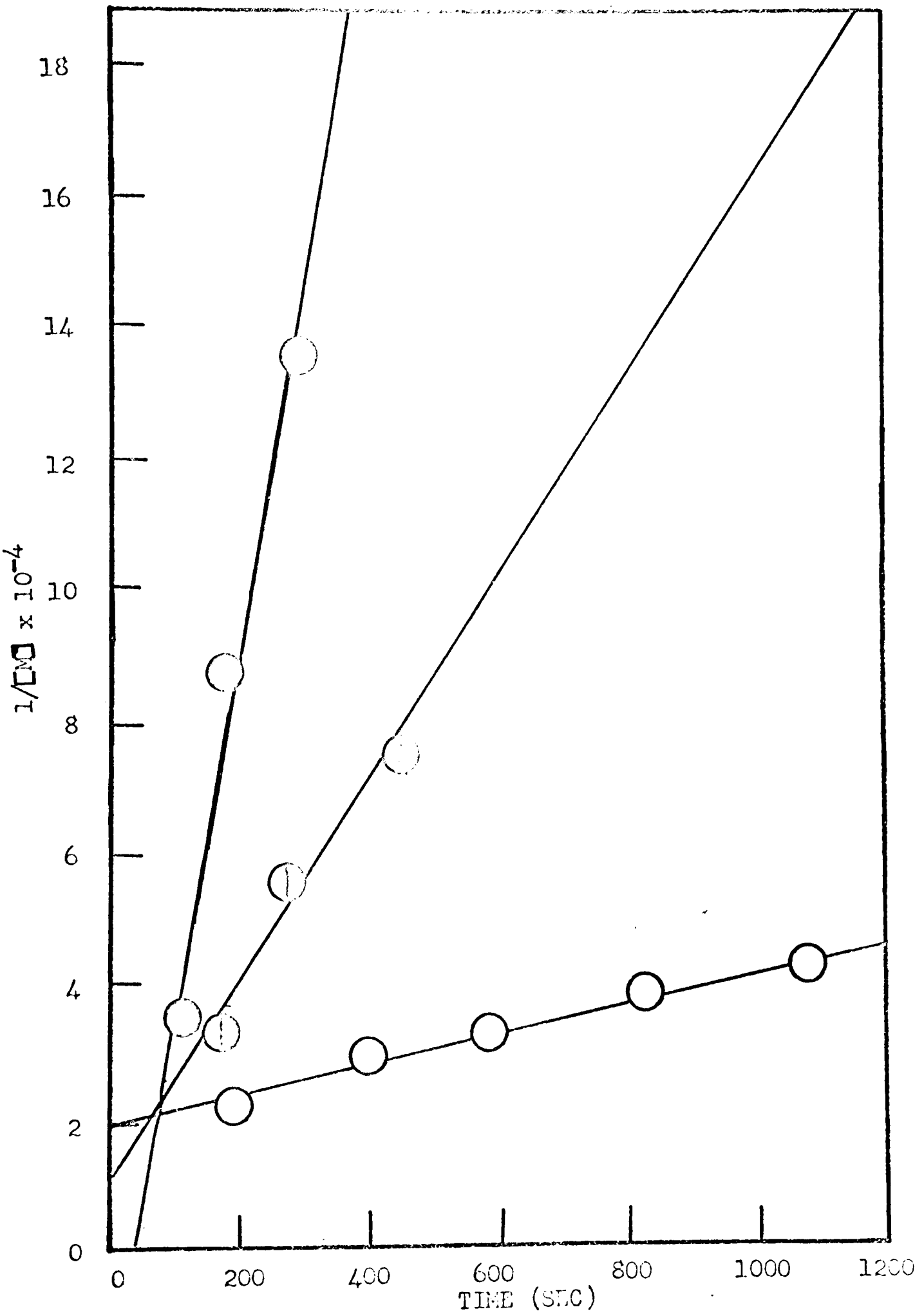
18
16
14
12
10
8
6
4
2
0
1/EM x 10⁻⁴
0
200
400
600
800
1000
1200
TIME (SEC)

$$K = A^* \, e^{-E_t^*/RT} \tag{82}$$

where A^* is the pre-exponential factor, and E_t^* is the activation energy. When the natural logarithm of both sides of Equation 82 is taken, the following is obtained:

$$\ln K = \ln A^* - E_t^*/RT. \tag{83}$$

Taking the derivative gives

$$d\ln K/d(1/T) = -E_t^*/R. \tag{84}$$

Therefore, a plot of lnK vs 1/T should be a straight line with a slope of $-E_t^*/R$ and an intercept of lnA*.

From the values of lnK and 1/T given in Table VII, such a plot was made and is shown in Figure 12. From the slope of the straight line, the activation energy was found to be

$$E_t^* = 94.7 \pm 8 \text{ Kcal/Mole} \tag{85}$$

and the pre-exponential factor was found to be

$$A^* = 2.5 \pm 1 \times 10^{60} \text{ mole}^{-1}\text{sec}^{-1}. \tag{86}$$

Using absolute reaction rate theory, $\Delta S^{\ddagger}$ was calculated to be

$$\Delta S^{\ddagger} = 58 \text{ cal/deg mole}. \tag{87}$$

From the gas-evolution curve (20) given in Figure 19 of Appendix E, page 115, it can be seen that the oxidation-reduction reaction of this compound occurs between 75-90° C. The reaction occurs after about one third of the hydrate-bound water has been evolved. To determine if the presence of the water played a part in the oxidation-reduction reaction, isothermal kinetic runs were made at temperatures of 50°, 57°, and 59° C. At these temperatures, according to the gas-evolution curve, the water should slowly be evolved but the oxidation-reduction reaction should not occur if the presence of the water does

FIGURE 12. Arrhenius Plot

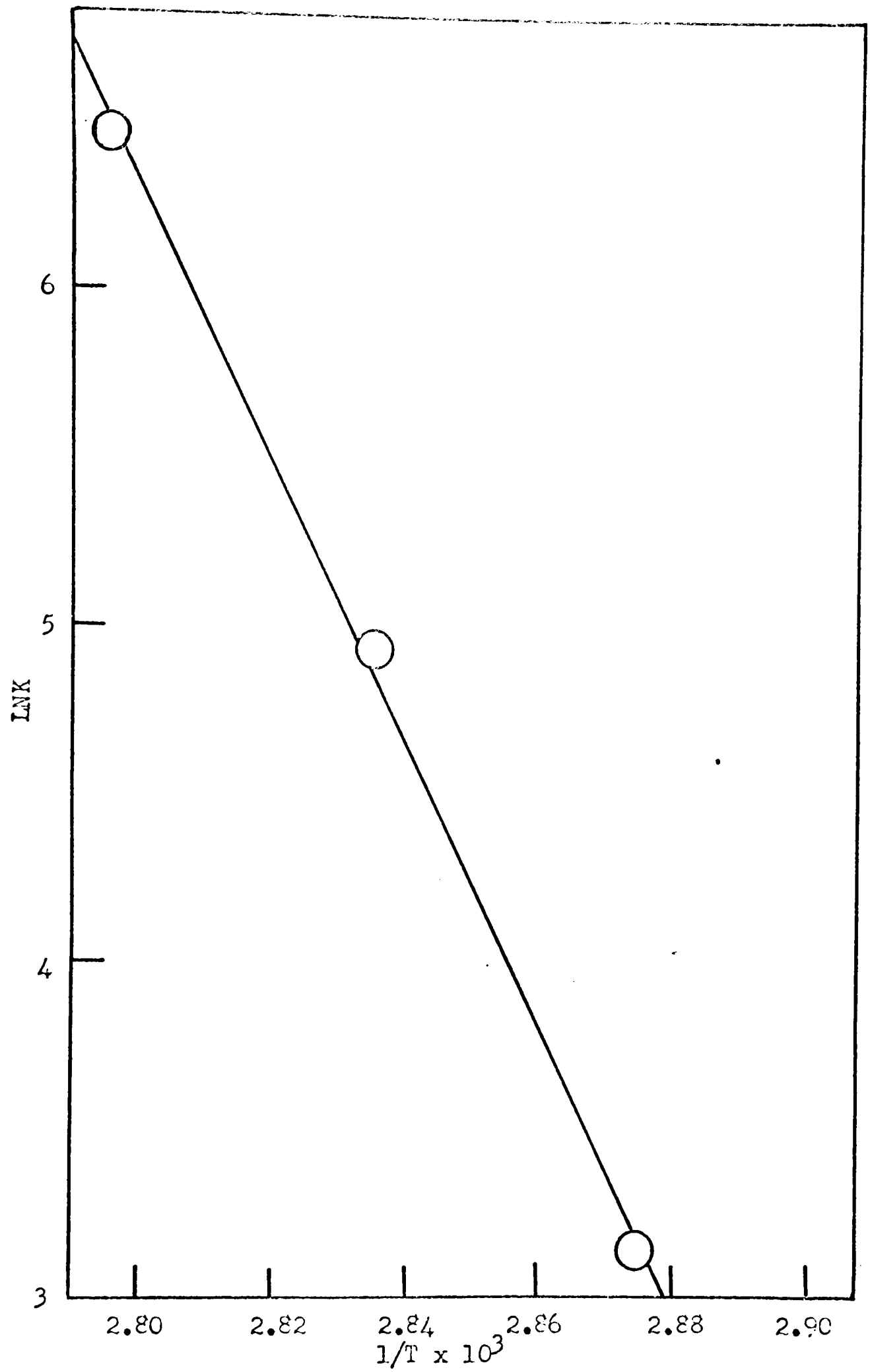
6
5
4
3
LNK
2.80
2.82
2.84
2.86
2.88
2.90
1/T x 10^3

not affect it. It was found, however, that small amounts of white product became visible after 50-60% of the water evolved, and the reaction continued after all of the water evolved. This indicates that the removal of some of the hydrate-bound water is necessary before the oxidation-reduction reaction can occur.

The first-order rate plots of the evolution of the hydrate-bound water prior to the oxidation-reduction reaction are given in Figure 21 of Appendix E, page 116, and the Arrhenius plot is given in Figure 22 of Appendix E, page 118. The activation energy for the removal of the water was found to be

$$E^* = 3 \pm 1 \text{ Kcal/mole.} \qquad (88)$$

The results of this investigation presented in this chapter are discussed in the following chapter.

CHAPTER V

DISCUSSION

A Possible Reaction Mechanism

Since the activation energy of the thermal oxidation-reduction reaction (Equation 85) of potassium tris(oxalato)manganate(III) 3-hydrate in the solid state is close in value to the average excitation energy (Equation 76) determined from photochemical data, it is safe to assume that the mechanisms of the two reactions are similar. Since one oxalate ion must reduce two metal ions, two molecules of reactant must ultimately be involved in the reaction mechanism. There are at least five possible mechanisms which result in the products given by Equation 1. These are listed below. In these equations

$$M = K_3[Mn(C_2O_4)_3]\cdot 3H_2O,\ P = K_2[Mn(C_2O_4)_2],\ C^* = C_2O^{\bullet -},$$
$$g = CO_2,\ p = K_2C_2O_4,\ M^* = K_3[(C_2O_4)_2MnOCOCOO:],$$
$$P^* = K_3[(C_2O_4)_2MnOCOCOO\bullet],\ \text{and}$$
$$M\text{-}M^* = K_6[(C_2O_4)_2MnOCOCOOMn(C_2O_4)_2OCOCOO:]. \qquad (89)$$

A. Bridged intermediate electron transfer,

$$M \rightleftharpoons M^*$$
$$M^* + M \longrightarrow M\text{-}M^* \longrightarrow 2P + p + 2g. \qquad (90)$$

B. Oxalate ion radical electron transfer,

$$M \rightleftharpoons P^* \longrightarrow P + C^*$$

$$C^* + M \longrightarrow P + 2g + p. \qquad (91)$$

C. Oxalate ion radical reaction,

$$2M \rightleftharpoons 2P^* \longrightarrow 2P + 2C^*$$

$$C^* + C^* \longrightarrow 2g + p. \qquad (92)$$

D. Attached oxalate ion radical reaction,

$$2M \rightleftharpoons 2P^*$$

$$P^* + P^* \longrightarrow 2P + p + 2g. \qquad (93)$$

E. Bridged radical electron transfer,

$$M \underset{K_{-1}}{\overset{K_1}{\rightleftharpoons}} P^*$$

$$P^* + M \xrightarrow{K_2} 2P + 2g + p. \qquad (94)$$

On the basis of the experimental evidence determined in this investigation, any postulated mechanism for the reaction given in Equation 1 must explain the following facts:

1. The thermal activation energy is the same as the average excitation energy.

2. The photochemical quantum yield is two.

3. The order of the thermal reaction is two.

4. The magnitude of the thermal activation energy is on the order of an electronic excitation.

5. The thermal pre-exponential factor is unusually large.

6.. The presence of the hydrate-bound water inhibits the thermal reaction.

Mechanism A is unlikely because it is doubtful that the breaking of a metal-ligand which requires 9 Kcal/mole would involve such a large activation energy as that found for the reaction given in Equation 1. Furthermore, crystal structure studies (56) reveal

that the manganese ions are not close enough together in the crystal lattice to allow the bridged intermediate to form.

Mechanisms B and C are unlikely because they involve the diffusion of the reactive species, C*, which would result in diffusion controlled or one half rather than second order kinetics.

Mechanisms C and D are unlikely because they would require a quantum yield of one rather than two. Furthermore, mechanism D requires the almost simultaneous excitation of two adjacent molecules, which is an improbable event.

Thus, only mechanism E is left as a probable mechanism for the reaction given in Equation 1. This mechanism does explain all of the observations concerning this reaction. Mechanism E is given in more detail below, where the potassium ions and the water have been omitted from the picture for clarity only:

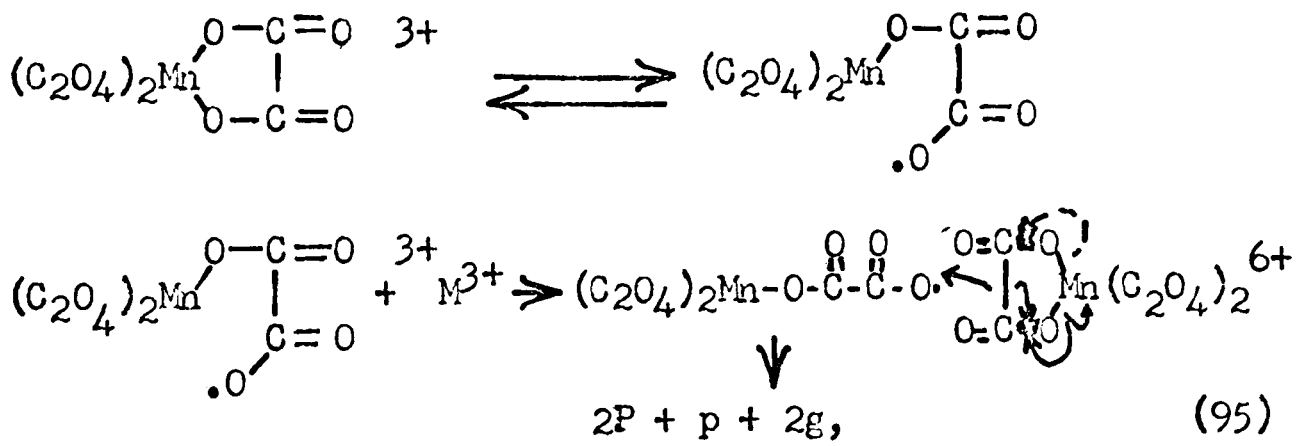

$$2P + p + 2g, \qquad (95)$$

where solid arrows represent the movement of single electrons and broken arrows represent the movement of electron pairs.

If it is assumed that the second step of Mechanism E is the rate controlling step of the thermal reaction, then the rate constant of the second step of the reaction mechanism, $\underline{K}_2$, is much smaller than the rate constants of the first step, $\underline{K}_1$ and $\underline{K}_{-1}$, or

$$K_1,\ K_{-1} >> K_2. \tag{96}$$

The equilibrium in the first step would then hold, or

$$K_1/K_{-1} = P^*/M \tag{97}$$

where $\underline{P}^*$ and $\underline{M}$ are now concentrations. The rate of production of the product, from the second step, is

$$dP/dt = 2K_2MP^* \tag{98}$$

When Equation 97 is rearranged and substituted into Equation 98, the following is obtained:

$$dP/dt = (2K_2K_1/K_{-1})\ M^2. \tag{99}$$

This explains the observed second order kinetics.

Mechanism E also explains the observed quantum yield of two. The absorption of one photon in the first step results in the production of two molecules of product, or

$$\phi = \frac{2 \text{ molecules of product}}{1 \text{ photon absorbed}} = 2. \tag{100}$$

From the Arrhenius equation,

$$K_2 = A_2^*\ e^{-E_2^*/RT} \tag{101}$$

and

$$K_1/K_{-1} = (A_1^*/A_{-1}^*)\ e^{-E^*/RT} \tag{102}$$

where $\underline{E}^*$ is the energy difference between $\underline{M}$ and $\underline{P}^*$ or the excitation energy. Substituting Equations 101 and 102 into Equation 99 gives

$$dP/dt = (2A_2^*A_1^*/A_{-1}^*)\ e^{-(E_2^* + E^*)/RT}\ M^2. \tag{103}$$

Since the second step is a free radical reaction, its activation energy would be expected to be small while the excitation energy is large so that

$$E^* \gg E_2^*. \tag{104}$$

Equation 103 therefore reduces to

$$dP/dt = (2A_2^*A_1^*/A_{-1}^*)\ e^{-E^*/RT}\ M^2 \tag{105}$$

which explains the fact that the thermal activation energy is the same as the actual average energy of excitation.

The presence of the hydrate-bound water probably inhibits the thermal reaction because its presence prevents the oxalate bridge in the second step of the mechanism. The question arises then as to whether its presence inhibits the second step in the photochemical reaction. Since the water is also evolved in the photochemical reaction (20), it is probably evolved in the excitation step (Equation 94). A further indication is the photochemical reaction of the corresponding chromium compound ($K_3[Cr(C_2O_4)_3]\cdot 3H_2O$). Although this compound does not undergo the oxidation-reduction reaction, it is dehydrated upon irradiation with ultraviolet radiation (54). Therefore, the second step of the reaction mechanism of $K_3[Mn(C_2O_4)_3]\cdot 3H_2O$ proceeds rapidly in the photochemical reaction because of the absence of the hydrate-bound water. The reaction induced photochemically is therefore first order with respect to reactant and little of the excited species, P*, undergoes the reverse reaction of the first step of the mechanism.

When the reaction is induced thermally, the second step of the mechanism , however, is inhibited by the presence of the hydrate-bound water. The second step is much slower in this case and much more of the reactive species undergoes the reverse reaction of the first step of the mechanism. The observed reaction order is therefore

two. Another indication of this is the activation energies. The activation energy of the thermal evolution of the water is about 3 Kcal/mole (Equation 88) and the activation energy of the thermal oxidation-reduction reaction is about 95 Kcal/mole (Equation 85). The sum of the two numbers is 98, close to the value of 100 Kcal/mole (Equation 76) for the photochemical excitation energy. These numbers further suggest that the evolution of the water and the excitation reaction occur simultaneously when the reaction is induced photochemically but that the two reactions occur in different steps when the reaction is induced thermally.

The reaction mechanism which has been presented here is also supported by studies of the crystalline structure of the compound, $K_3[Fe(C_2O_4)_3] \cdot 3H_2O$, which is isomorphous with $K_3[Mn(C_2O_4)_3] \cdot 3H_2O$ (56). The positions of the atoms in the determined structure are such that the oxalate bridging step can occur if the hydrate-bound water is removed. The water of hydration is in a position such that the oxalate radical cannot come into contact with a neighboring anion.

The one remaining fact that has not yet been explained is the unusually large value of the observed pre-exponential factor of the thermal reaction. However, there is nothing with which to compare it. There have been no previous investigations of solid-state oxidation-reduction reactions interpreted on the basis of a chemical mechanism. Compared to usual values of pre-exponential factors of gaseous and liquid reactions, however, the value obtained in this investigation is unusually large.

Ordinary gaseous and liquid reactions seldom involve changes of state, and the entropy changes are therefore small. Since the pre-exponential factor is related to the entropy changes by the absolute reaction rate equation, small pre-exponential factors are expected. The reaction studied in this investigation, however, is a solid-state reaction and changes of state are involved. Water goes from bound water to gaseous water, and an oxalate ion reacts to give two molecules of gaseous carbon dioxide. The large values of the entropy changes of these processes are indicated by the entropy changes of the similar reactions given below: (57)

$$C_2O_4^{2-}(\text{Aqueous}) \longrightarrow 2CO_2 \qquad \Delta S = 90 \text{ cal/deg mole} \quad (106)$$

$$H_2O\ (\text{Solid}) \longrightarrow H_2O\ (\text{Gas}) \qquad \Delta S = 28 \text{ cal/deg mole.} \quad (107)$$

It is not clear whether or not the entropy of the evolution of the water is involved in the entropy of activation. However, the entropy change given by Equation 106 must be involved. Since one oxalate ion is oxidized when two manganese ions are reduced, one half of the value given by Equation 106 should contribute to the entropy of activation. This gives a value of 45 cal/deg mole which is concordant with the value of 58 cal/deg mole (Equation 87) which was found for the reaction studied in this investigation. Since the value of 45 was obtained for oxalate ions in aqueous soultions, it would be expected to be lower in value than for solid-state oxalate ions.

The reaction mechanism of the solid-state oxidation-reduction reaction of potassium tris(oxalato)manganate(III) 3-hydrate which

has been presented here explains all of the observed facts concerning both the thermal and the photochemical reactions. It appears that these reactions proceed by the same mechanism. The data obtained from the photochemical studies helped much in the determination of the reaction mechanism. From them, the value of the excitation energy and the number of product molecules obtained for each reactant molecule which was excited were determined. This information along with the thermal reaction data allowed the postulation of the common mechanism.

Comparisons

The mechanisms of the solid-state reactions of potassium tris-(oxalato)manganate(III) 3-hydrate were found to be different than those of its reactions in aqueous solutions. In aqueous solutions, the electron transferring species was postulated to be an oxalate ion radical (40). It is doubtful that such a species could exist freely in the solid state where there would be no solvent molecules to stabilize it. The activation energy of the reaction in solution is only about one fourth as large as that of the solid-state reaction (40). This is understandable, however, since the reaction mechanisms are different. In aqueous solutions, the first step of the reaction is thought to be the replacement of the labile oxalate ligand by two molecules of water

$$Mn(C_2O_4)_3^{3-} + 2H_2O \longrightarrow Mn(C_2O_4)_2(H_2O)_2^{-} + C_2O_4^{2-}. \qquad (108)$$

The resulting bis(oxalato) compound is very unstable toward oxidation-reduction and will react at about room temperature. It then undergoes an oxidation-reduction reaction. Thus a different compound undergoes the actual reaction in solution than in the solid state.

For the series of compounds, $K_3[M(C_2O_4)_3]\cdot 3H_2O$ (M = Mn, Co, Fe, Cr), in the solid state, the Mn, Co, and Fe compounds undergo an oxidation-reduction reaction in which the metal ion is reduced from the trivalent to the divalent oxidation state both thermally and photochemically (19-22). The chromium compound does not. Furthermore, the reaction temperatures of the thermal reactions of the compounds increase in the order Mn < Co < Fe. This is also the order of decreasing rates of the photochemical reactions. This can be explained by the oxidation potentials (55):

$$M^{2+} \longrightarrow M^{3+} \qquad \begin{array}{l} Mn = 1.54\ V \\ Co = 1.84\ V \\ Fe = 0.77\ V \\ Cr = -.04\ V. \end{array} \qquad (109)$$

There appears to be a reverse in the expected order between Mn and Co. This is explained, however, by the difference in the stabilization energies of these two ions upon coordination. The d orbitals of octahedral complexes of Co(III) and Mn(III) oxalato complexes are occuppied as shown below:

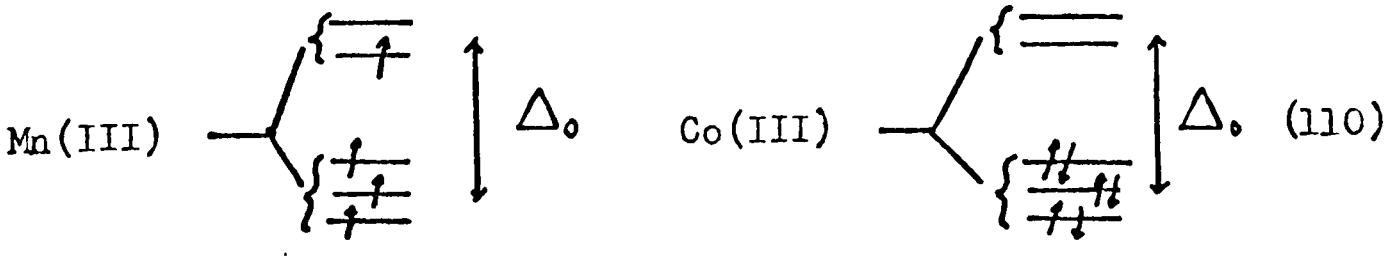

(110)

The cobalt compound is a low spin complex while the manganese

compound is a high spin complex. The reason is that Δ_o for Co(III) is larger than the electron pairing energy and it is less for Mn(III). The stabilization energies are

$$\text{Mn(III)} \quad \text{S. E.} = 3(2/5)\Delta_o - (3/5)\Delta_o = (3/5)\Delta_o \tag{111}$$

$$\text{Co(III)} \quad \text{S. E.} = 6(2/5)\Delta_o = (12/5)\Delta_o. \tag{112}$$

The Δ_o's as calculated from spectral data are

$$\text{Co(III)} \qquad \Delta_o = 60 \text{ Kcal/mole} \tag{113}$$

$$\text{Mn(III)} \qquad \Delta_o = 53 \text{ Kcal/mole}. \tag{114}$$

Therefore, the stabilization energies are

$$\text{Co(III)} \qquad \text{S. E.} = 144 \text{ Kcal/mole} \tag{115}$$

$$\text{Mn(III)} \qquad \text{S. E.} = 32 \text{ Kcal/mole}. \tag{116}$$

The cobalt complex is thus much more stable than the corresponding manganese complex.

The cobalt, manganese, and iron oxalato complexes undergo oxidation-reduction reactions because the trivalent metal ions are good oxidizing agents and the oxalate ion is a good reducing agent.

Both Mn(III) and Co(III) ions are so unstable toward reduction that they can only exist as complex ions. There are many stable Co(III) complexes, because, as noted previously, its stabilization energy is large. There are, however, very few stable Mn(III) complexes. It has such a small stabilization energy and it is so easily reduced that only the strong field ligands such as cyanide ions can form appreciably stable complexes.

From this investigation, it appears that the hydrate-bound water has a stabilizing effect against the oxidation-reduction reaction

of the oxalato manganese(III) compound, which appears to be caused by an inhibition against the formation of an oxalate ion bridge between two molecules. The electron transfer is inhibited and the reaction cannot take place with the water present. The complex, $K_3[Mn(C_2O_4)]\cdot 3H_2O$, is therefore stable in the solid state only in the dark with the presence of the hydrate-bound water at temperatures lower than those required to remove the water.

Manganese(III) ions appear to prefer oxygen ligands instead of nitrogen ligands. No compounds containing manganese(III)-nitrogen bonds have been reported, while the hydrated oxalate and malonate complexes do exist. The complex with the strongest ligand known (cyanide ion) is stable toward oxidation-reduction except at high temperatures (58). In binary compounds, such as the halides, the manganese(III) ion exibits the expected similar behavior. The compound, MnF_3, is stable, the compound, $MnCl_3$, is unstable, and the compounds, $MnBr_3$ and MnI_3, do not appear to exist. The fluoride ion is not a reducing agent, the chloride ion is a better, but poor reducing agent, and the bromide and iodide ions are relatively good reducing agents. The stability of manganese(III) compounds appears to depend mostly on the field strength and the reducing ability of the ligands. It is safe to predict that complexes of manganese(III) with such ligands as sulfite ions would probably not exist even though manganese(III) prefers oxygen ligands because sulfite ions are good reducing agents. Other oxygen bonding ligands that are not good reducing agents such as carbonate ions should form complexes with manganese(III) ion at very low temperatures.

They would probably not exist at room temperatures, however, because carbonate ion is not a strong ligand and if it is bidentate, it must undergo considerable ring strain to form the necessary four membered rings.

There are many oxidation-reduction reactions of transition metal coordination compounds in the solid state which involve the transfer of electrons between ions or molecules. It is likely that such reactions involve mechanisms similar to that of the reaction studied in this investigation. They must involve an excitation step and a step involving some method of transfering electrons. The relative stabilities and therefore the relative reaction temperatures of such compounds can be qualitatively explained on the basis of the complexing stabilization energy, the oxidation potentials of the central metal ions, and the reduction potentials of the reducing ligands.

Furthermore, from this investigation, it appears that the thermal activation energies of such reactions can be approximated from the excitation energies (the energy corresponding to the wavelength of their charge transfer band). Also, it appears possible to estimate the relative magnitudes of the pre-exponential factors from the amount of changes of phase involved in the reactions.

It appears that a general prediction may be made as to which coordination compounds will undergo photochemical oxidation-reduction reactions. Any coordination compound which has

1. a metal ion with an unfilled orbital,

2. a metal ion unstable with respect to a lower oxidation state, and

3. ligands which are good reducing agents will probably undergo photochemical oxidation-reduction reactions. These reactions should occur under radiation corresponding in energy to the charge transfer bands of the compounds.

Other solid-state thermal reaction kinetics which have been studied have been explained on the basis of physical rather than chemical processes. Probably the reason that the kinetics of the reaction given in Equation 1 were chemically controlled was that the activation energy of the excitation step was much larger than that of any physical process which may be involved, such as nucleus formation and growth. Thus it appears that if a chemical step has a large enough activation energy, it rather than some physical step will be the kinetic rate controlling reaction of a solid-state mechanism.

CHAPTER VI

CONCLUSIONS

1. Using a modified Beer-Lambert equation and considering a photochemical reaction to be a bimolecular reaction between a molecule of a reactant and a photon, the following equation was derived to describe the rate of a photochemical reaction of a powdered sample:

$$d\alpha'/dt = \frac{aI_o\lambda\phi\epsilon_r(1-\alpha')\,e^{-Ux}}{hcN_o} - V\int_0^x \alpha' dx.$$

By assuming that x is very small, the Lambert cosine law for mat surfaces is valid for powdered samples, and the solution values of the absorption coefficients are the same as the solid-state values, this equation can be used in the following form for photochemical reactions of powdered samples:

$$d\alpha/dt = I_o\lambda\phi\epsilon_r(1-\alpha)/hcN_o\pi.$$

2. This equation was applied to the solid-state photochemical reaction of potassium tris(oxalato)manganate(III) 3-hydrate. The experimental rate of reaction of this compound corresponds well with the derived equation. Using this equation and the experimental results, the quantum yield of this reaction was found to be $1.99 \pm .17$, close to the expected value of two.

3. Reflectance spectroscopy appears to be a very good method

of measuring the extent of reaction of a photochemical reaction of a powdered sample. Although the actual amount reacted at any time and the total amount which can react are not known, the fraction of the total amount which can react, reacted at any time can be determined. This is made possible by the use of a correction factor, γ, which was derived from reflectance equations.

4. The rate of the solid-state photochemical reaction of potassium tris(oxalato)manganate(III) 3-hydrate was found to increase exponentially with the reciprocal of the wavelength of the radiation up to a maximum value, beyond which it sharply decreased. This exponential dependence is thought to arise from a Boltzmann distribution of the population of the energy levels. The average excitation energy was found to be 100 ± 4 Kcal/mole.

5. The solid-state thermal reaction of potassium tris(oxalato)-manganate(III) 3-hydrate was found to be second order with respect to reactant. The activation energy was found to be 94.7 ± 8 Kcal/mole, and the pre-exponential factor was found to be $2.5 \pm 1 \times 10^{60}$ $(\text{mole sec})^{-1}$. The hydrate-bound water inhibited the thermal reaction.

6. The following mechanism was postulated for the thermal and the photochemical reactions of potassium tris(oxalato)manganate(III) 3-hydrate in the solid state:

$$M \rightleftharpoons P^*$$

$$P^* + M \longrightarrow 2P + p + 2\varepsilon.$$

This mechanism explained all of the observed facts concerning the reaction.

7. The mechanisms of the solid-state and solution reactions of potassium tris(oxalato)manganate(III) 3-hydrate are different.

8. The manganese(III) ion appears to be unstable and will exist only under certain specific conditions. It must be complexed with ligands which are strong and not readily reduced. If it is complexed with weak or readily reduced ligands, the crystal structure must incorporate such barriers as water of hydration.

9. It is likely that many solid-state oxidation-reduction reactions of transition metal coordination compounds which involve the transfer of electrons between molecules involve reaction mechanisms similar to that determined for the compound studied in this investigation.

10. The relative stabilities of coordination compounds toward oxidation-reduction can be qualitatively explained on the basis of ligand field theory and the oxidation and reduction potentials of the ligands and the central metal ions.

11. The activation energies and pre-exponential factors of these reactions can be estimated on the basis of the positions of the charge transfer bands and the amount of changes of state.

12. Transition metal coordination compounds which contain metals with unfilled orbitals which are easily reduced and ligands which are easily oxidized will probably undergo photochemical and thermal oxidation-reduction reactions.

13. If a chemical step of a solid-state reaction has a large enough activation energy, it will probably be the rate controlling

step rather than some physical process such as diffusion or nucleus formation and growth.

LIST OF REFERENCES

1. G. K. Rollefson and M. Burton, "Photochemistry", Prentice-Hall Inc., N. Y., (1946), p1.

2. Draper, Phil. Mag. 19, 195, (1841).

3. Stark, Physik Z. 9, 889 (1905).

4. Stark, Ann. Physik 38, 467 (1912).

5. Einstein, Ann. Physik 37, 832 (1912).

6. Einstein, J. Phys. 3, 277 (1913).

7. H. Shaw and S. Toby, J. Chem. Ed. 43, 408 (1966).

8. W. W. Wendlandt and H. G. Hecht, "Reflectance Spectroscopy", Interscience Publishers, N. Y., (1966), p59.

9. F. A. Cotton and G. Wilkinson, "Advanced Inorganic Chemistry", Interscience Publishers, N. Y., (1966), p713.

10. A. W. Adamson, "Spectrospecific Photolysis of $Cr(en)_2(OH)_2^+$ Ion, Mechanisms of Inorganic Reactions", Am. Chem. Soc. Publications, Washington, (1965), p237.

11. A. W. Adamson, Dis. Faraday Soc. 29, 163 (1960).

12. D. A. Young, "Decomposition of Solids, The International Encyclopedia of Physical Chemistry and Chemical Physics", Pergamon Press, London, (1966), p8.

13. W. E. Garner, "Chemistry of the Solid State", Butterworth's Scientific Publications, London, (1955).

14. G. Watt, Inorg. Chem. 3, 325 (1960).

15. N. Tanako and M. Nanjo, Bull. Chem. Soc. Japan 37, 1330 (1964).

16. E. L. Simmons and W. W. Wendlandt, J. Inorg. Nucl. Chem. 28, 2187 (1966).

17. E. L. Simmons and W. W. Wendlandt, J. Inorg. Nucl. Chem. 28, 2437 (1966).

18. W. W. Wendlandt and L. K. Sveum, J. Inorg. Nucl. Chem. 28, 393 (1966).

19. W. W. Wendlandt and E. L. Simmons, J. Inorg. Nucl. Chem. 27, 2317 (1965).

20. E. L. Simmons and W. W. Wendlandt, J. Inorg. Nucl. Chem. 27, 2325 (1965).

21. W. W. Wendlandt and E. L. Simmons, J. Inorg. Nucl. Chem. 28, 2420 (1966).

22. E. L. Simmons, Master's Thesis, Texas Technological College, 1966.

23. W. W. Wendlandt and J. H. Woodlock, J. Inorg. Nucl. Chem. 27, 259 (1965).

24. C. H. Stembridge and W. W. Wendlandt, J. Inorg. Nucl. Chem. 27, 129 (1965).

25. S. K. Deb and A. D. Yoffe, Proc. Roy. Soc. A254, 528 (1960).

26. S. K. Deb and A. D. Yoffe, Proc. Roy. Soc. A254, 5.5 (1960).

27. D. A. Young, "Decomposition of Solids, The International Encyclopedia of Physical Chemistry and Chemical Physics", Pergamon Press, London, (1966), p110.

28. R. J. Kern, J. Am. Chem. Soc. 75, 1965 (1963).

29. N. V. Sidgwick, "The Chemical Elements and Their Compounds", Oxford University Press, Oxford, (1950), Vol. II p1279.

30. S. E. Beacom, Doctoral Dissertation, University of Connecticut, 1954.

31. T. Onescu, Acad. Rep. Populare Romine, Studii cercetari chim. 8, 237 (1960).

32. M. Matsui and T. Naksiski, J. Research Inst. 46, 26 (1952).

33. N. A. Bisikalova, Ukrain Kim. Shur. 17, 807 (1951).

34. T. B. Copestake and N. Uri, Proc. Roy. Soc. A228, 252 (1955).

35. J. Hatchett and R. Marcus, Arch. Biochem. Biophys. 76, 233 (1958).

36. C. A. Parker, Trans. Faraday Soc. 50, 1213 (1954).

37. C. A. Parker and C. C. Hotchort, J. Phys. Chem. 63, 22 (1959).

38. K. V. Krishnamurity and C. M. Harris, Chem. Rev. 61, 213 (1961).

39. B. K. Muderji and N. R. Dhar, J. Indian Chem. Soc. 5, 203 (1928).

40. I. G. Murgulescu and T. Onsescu, Revue Roumaine de Chimie 10, 3 (1965).

41. G. H. Cartledge and W. P. Ericks, J. Am. Chem. Soc. 58, 2061 (1936).

42. T. R. Griffiths, Anal. Chem. 35, 1077 (1963).

43. W. W. Wendlandt and H. G. Hecht, "Reflectance Spectroscopy", Interscience Publishers, N. Y.,, (1966).

44. E. L. Simmons and W. W. Wendlandt, Anal. Chem. Acta 461, 35 (1966).

45. P. W. Selwood, "Magnetochemistry", Interscience Publishers, N. Y., (1943), p98.

46. P. W. Selwood, "Magnetochemistry", Interscience Publishers, N. Y., (1943), p8.

47. P. W. Selwood, "Magnetochemistry", Interscience Publishers, N. Y., (1943), p29.

48. W. W. Wendlandt and H. G. Hecht, "Reflectance Spectroscopy", Interscience Publishers, N. Y., (1966),p62.

49. J. H. Lambert, "Photometria sive de mensura it grodikus luminis colorum it umbrae", Augustae Vindelicarum, 1960.

50. W. W. Wendlandt and H. G. Hecht, "Reflectance Spectroscopy", Interscience Publishers, N. Y., (1966), p16.

51. H. Wright, Ann. Physik 1, 17 (1900).

52. G. H. Cartledge and W. P. Ericks, J. Am. Chem. Soc. 58, 2065 (1936).

53. D. P. Graddon, J. Inorg. Nucl. Chem. 3, 308 (1956).

54. E. L. Simmons, Unpublished work.

55. R. B. Heslop and P. L. Robinson, "Inorganic Chemistry", Elsevier Publishing Co., London, (1960).

56. P. Herpin, Bull. Soc. franc. Miner. Crist., 245 (1958).

57. F. T. Wall, "Chemical Thermodynamics", W. H. Freeman and Co., London, (1956), Appendix D.

58. F. A. Cotton and G. Wilkinson, "Advanced Inorganic Chemistry", Interscience Publishers, London, (1962), p708.

APPENDIX

A. The Rate Equation for the Photochemical Reaction of an Opaque Crystal

B. The Rate Equation for the Photochemical Reaction of a Transparent Crystal

C. Photochemical Rate Plots

D. Photochemical Kinetic Data

E. Thermal Data Plots

APPENDIX A: THE RATE EQUATION FOR THE PHOTOCHEMICAL REACTION OF AN OPAQUE CRYSTAL

Consider a beam of monochromatic radiation of intensity, I, which strikes a solid opaque surface of a material, A, which reacts to give a solid material, B. The intensity is the amount of energy impinging upon the surface per unit area in unit time, or

$$I = nhcN_o/\lambda \qquad \text{(A-1)}$$

where n is the number of einsteins of photons impinging upon unit area in unit time, h is Planck's constant, c is the velocity of light, and λ is the wavelength of the radiation.

For the reaction

$$A \xrightarrow{h\nu} B, \qquad \text{(A-2)}$$

if it is considered to be a bimolecular reaction between a molecule of A and a photon, then the following rate equation can be written:

$$-d[A]/dt = \beta[A]n \qquad \text{(A-3)}$$

where [A] is the concentration of A expressed in moles per unit area and β is the cross section of A and is given by

$$\beta = \epsilon\phi \qquad \text{(A-4)}$$

where ϵ is the absorption coefficient of A and ϕ is the quantum yield of the reaction given by Equation A-2.

Combinating Equations A-3 and A-4 gives

$$-d[A]/dt = \epsilon\phi[A]n. \qquad \text{(A-5)}$$

Rearranging Equation A-1 gives

$$n = I\lambda/hcN_o. \qquad (A-6)$$

Substitution of Equation A-6 into Equation A-5 gives

$$-d[A]/dt = \epsilon \phi I \lambda [A]/hcN_o. \qquad (A-7)$$

This is the rate equation for the photochemical reaction of an opaque crystal sample, A.

Rearranging and integrating Equation A-7 gives

$$\ln[A] - \ln[A_o] = -\phi\epsilon\lambda It/hcN_o \qquad (A-8)$$

where $[A_o]$ is the original concentration of A. Or,

$$\ln[A]/[A_o] = \ln(1 - \alpha) = -\epsilon\phi\lambda It/hcN_o \qquad (A-9)$$

where α is the fraction reacted.

Differentiation gives

$$d\ln(1 - \alpha)/dt = -\epsilon\phi\lambda I/hcN_o. \qquad (A-10)$$

Therefore, the slope of a plot of $\ln(1 - \alpha)$ vs t is a constant which is given by Equation A-10. Since h and c are constants, if I and λ are known, the value of $\epsilon\phi$ can be determined from such a plot. If ϕ is known, then ϵ can be calculated or if ϵ is known, then ϕ can be calculated.

APPENDIX B: THE RATE EQUATION FOR THE PHOTOCHEMICAL REACTION OF A TRANSPARENT CRYSTAL

Consider a semi-transparent solid sample with a thickness L. This sample is irradiated with monochromatic radiation with a wavelength of λ and an intensity of I_o.

A molecule of this sample, R, absorbs a photon to produce an excited species, R*,

$$R \xrightarrow{h\nu} R^*. \qquad \text{(B-1)}$$

If the reaction is considered to be a bimolecular reaction between a molecule of the reactant and a photon, then the following rate equation can be written:

$$-d[R]/dt = \beta[R]n \qquad \text{(B-2)}$$

where [R] is the concentration of the reactant in moles/cm^3 and

$$n = I\lambda/hcN_o. \qquad \text{(B-3)}$$

Substitution of Equation B-3 into Equation B-2 gives

$$-d[R]/dt = \beta\lambda[R]I/hcN_o. \qquad \text{(B-4)}$$

The radiation decreases as it passes through the sample according to Beer's law:

$$-dI = I\epsilon[R]dx. \qquad \text{(B-5)}$$

If the radiation strikes the surface of the sample at an angle of 90°, then the surface reflection is very small and can be neglected.

Equation B-5 cannot be integrated because [R] varies with the depth, x, into the sample. However, if the concentration is expressed

in moles per unit area, it is independent of the depth. Then

$$[R] = [R]'/L \tag{B-6}$$

where $[R]'$ is expressed in units of moles per unit area. Then

$$-dI = \epsilon I[R]'dx/L \tag{B-7}$$

and

$$\int_{I_o}^{I} dI/I = \epsilon[R]' \int_{0}^{L} dx/L \tag{B-8}$$

or,

$$\ln(I/I_o) = -\epsilon[R]'. \tag{B-9}$$

Taking the exponent of both sides of Equation B-9 gives

$$I = I_o\, e^{-\epsilon[R]'}. \tag{B-10}$$

Substitution of Equation B-6 into Equation B-4 gives

$$-d[R]'/dt = \beta[R]'I\lambda/hcN_o. \tag{B-11}$$

Substitution of Equation B-10 into Equation B-11 gives

$$-d[R]'/dt = ([R]'I_o\beta\lambda/hcN_o)\, e^{-\epsilon[R]'}. \tag{B-12}$$

Since,

$$\beta = \epsilon\phi \tag{B-13}$$

then

$$-d[R]'/dt = (\epsilon\phi\lambda[R]'Io/hcN_o)\, e^{-\epsilon[R]'}. \tag{B-14}$$

Taking the ln of both sides of Equation B-14 and differentiating gives

$$d\ln(\text{rate})/\left(d\ln[R]' - \epsilon[R]'\right) = 1. \tag{B-15}$$

Thus, a plot of ln(rate) vs $\ln[R]' - \epsilon[R]'$ gives a straight line with a slope of one and an intercept of $\ln(\epsilon\phi\lambda I_o/hcN_o)$. Therefore, if I_o, ϵ, and λ are known, the quantum yield, ϕ, can be determined from such a plot.

APPENDIX C: PHOTOCHEMICAL RATE PLOTS

FIGURE 13. Rate Plot (400 mμ)

Intensities (erg/cm^2 sec)

3.0 x 10^4 O

6.1 x 10^4 ❷

1.0 x 10^5 ❶

8.0 x 10^4 ❸

1.2 x 10^5 ⊙

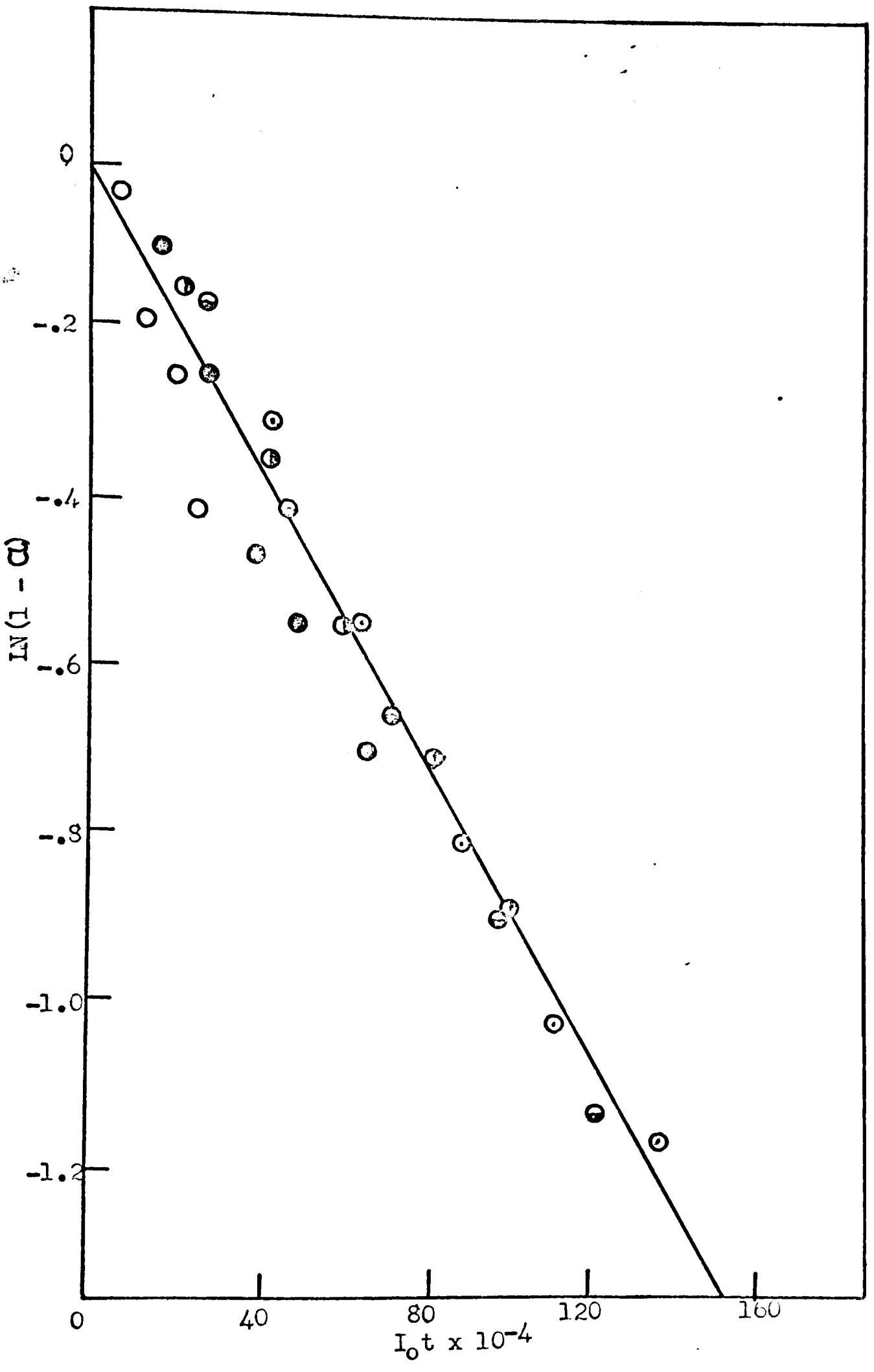
0
-.2
-.4
-.6
-.8
-1.0
-1.2
LN(1 - α)
0
40
80
120
160
$I_o t \times 10^{-4}$

FIGURE 14. Rate Plot (375 mμ)

Intensities (erg/cm^2 sec)

3.7×10^4 ○

5.2×10^4 ◉

7.5×10^4 ◐

8.6×10^4 ◒

1.2×10^5 ⊙

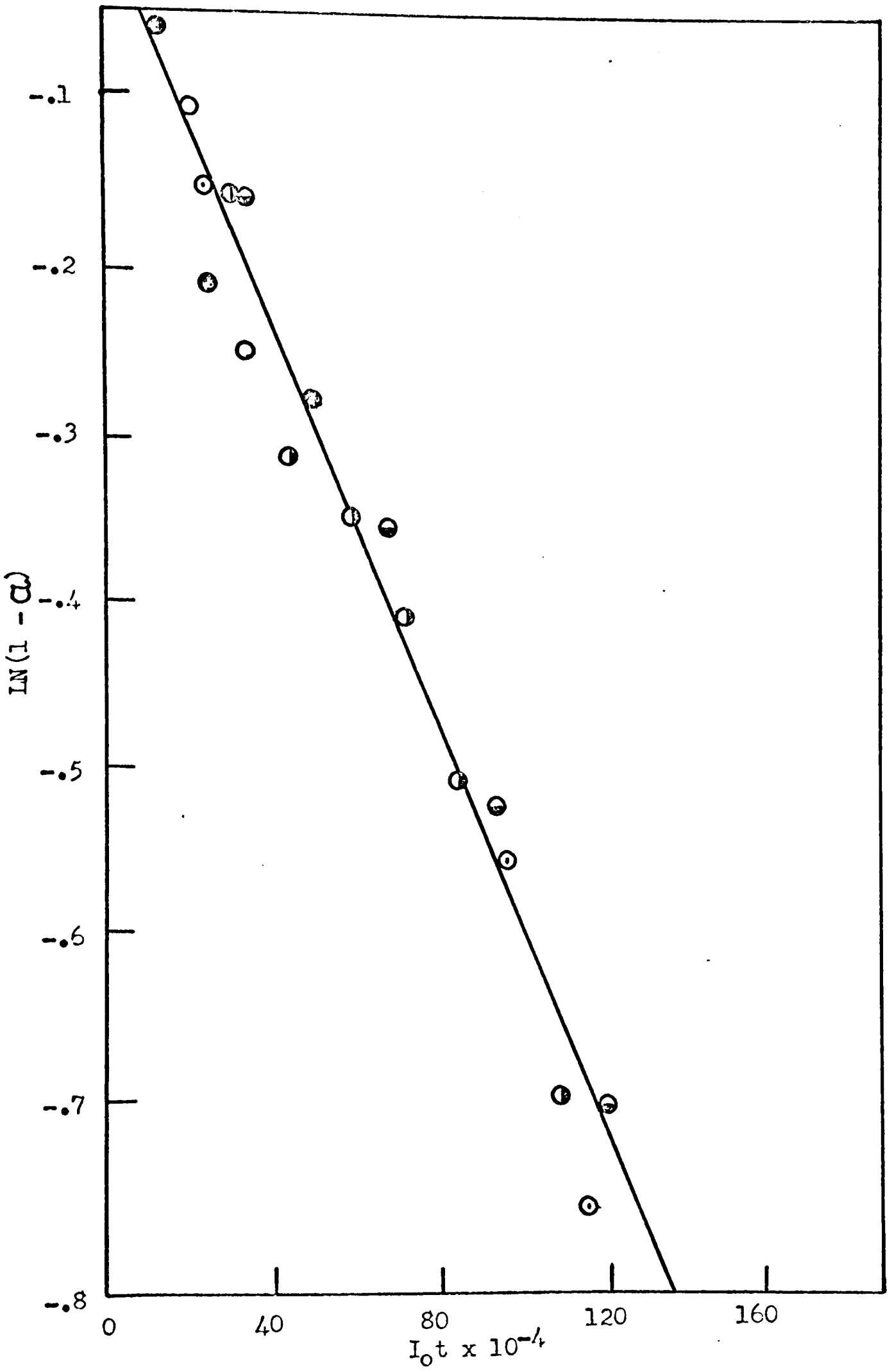
-.1
-.2
-.3
-.4
-.5
-.6
-.7
-.8
LN(1 - α)
0
40
80
120
160
$I_o t \times 10^{-4}$

FIGURE 14. Rate Plot (325 mμ)

Intensities (erg/cm^2 sec)	
1.0×10^4	Q
1.8×10^4	◐
2.7×10^4	●
4.0×10^4	⊙
6.0×10^4	◒

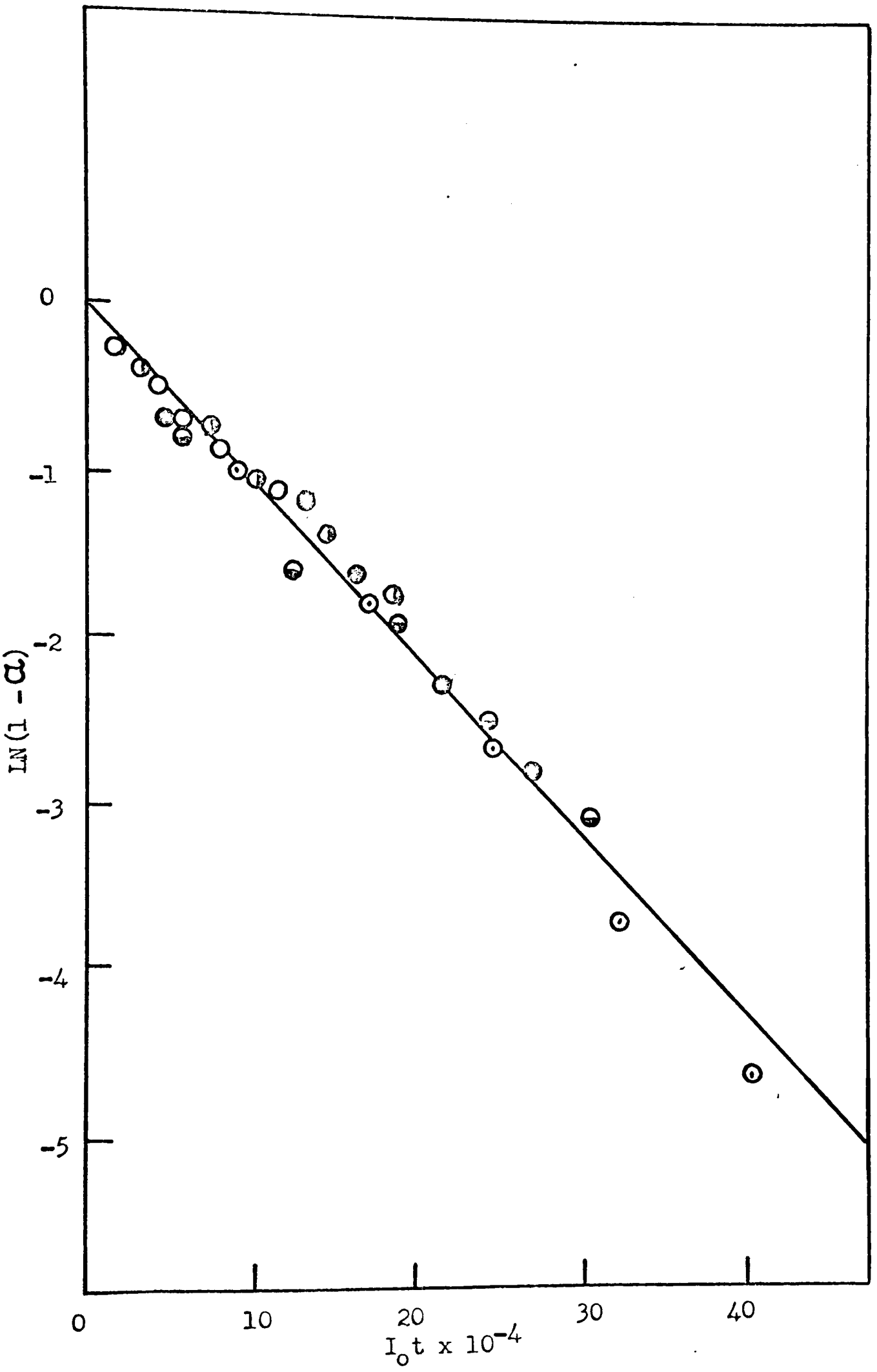
0
-1
-2
-3
-4
-5
LN(1 - α)
0
10
20
30
40
$I_o t \times 10^{-4}$

FIGURE 16. Rate Plot (300 mμ

Intensities (erg/cm^2 sec)

2.9×10^3 O

8.6×10^3 ◐

1.1×10^4 ◕

1.2×10^4 ⊙

1.4×10^4 ◒

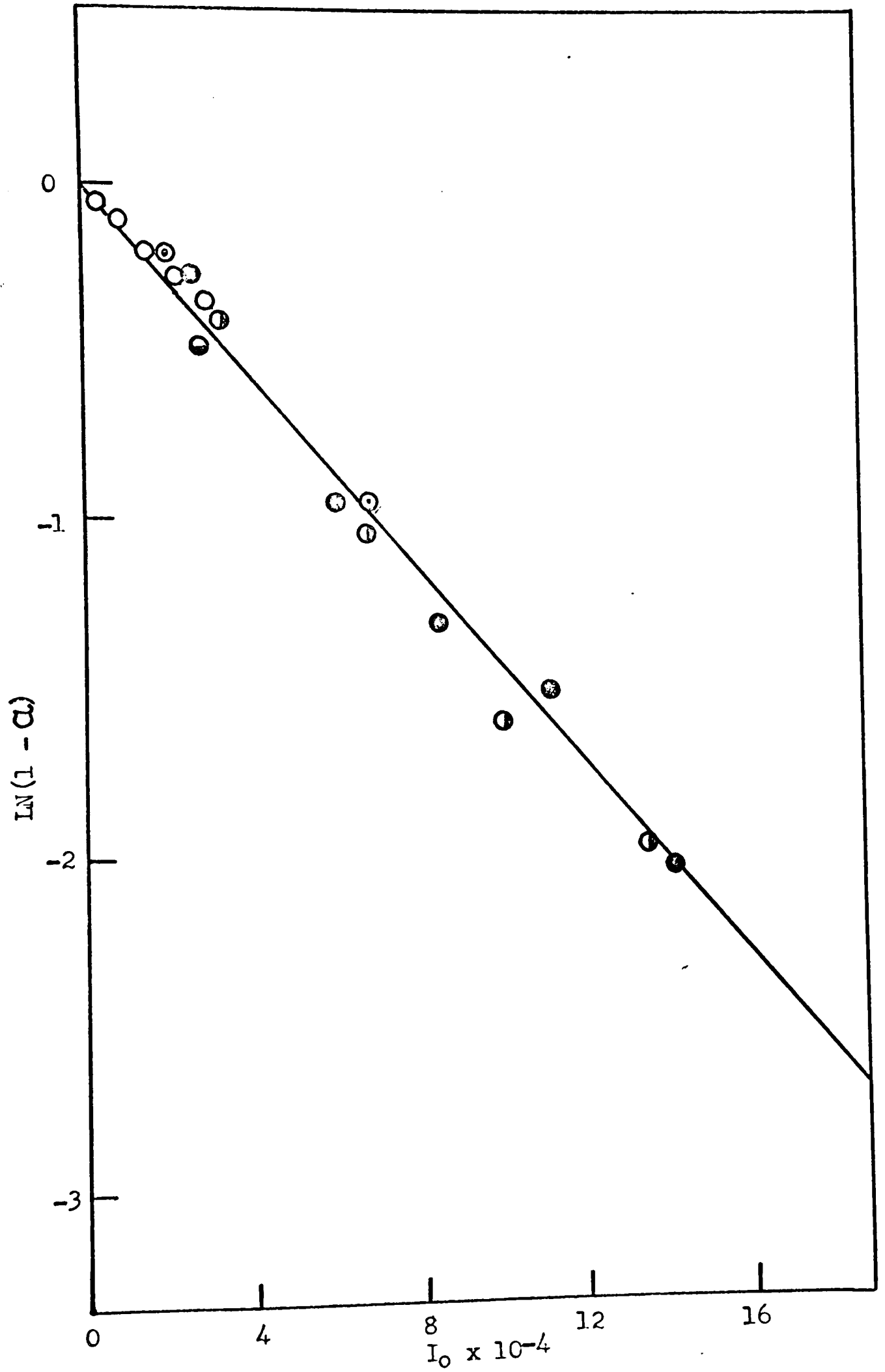
0
-1
-2
-3
LN(1 - C)
0
4
8
12
16
I_o x 10^{-4}

FIGURE 17. Rate Plot (275 mμ)

Intensities (erg/cm^2 sec)

5.1×10^3 ○

8.4×10^3 ◔

1.3×10^4 ◑

1.8×10^4 ◒

2.2×10^4 ◎

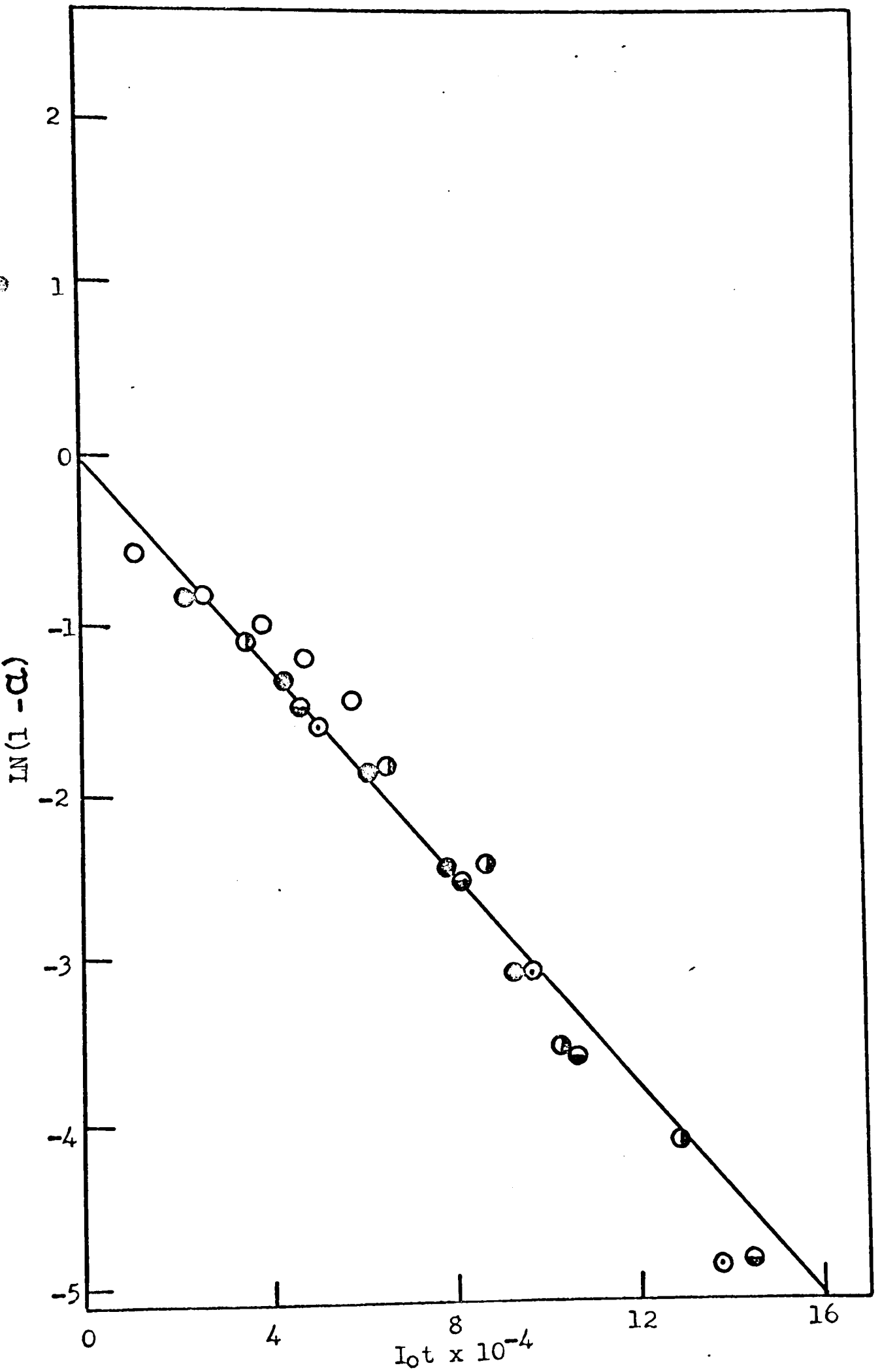
2
1
0
-1
-2
-3
-4
-5
LN(1 -α)
0
4
8
12
16
$I_o t \times 10^{-4}$

FIGURE 18. Rate Plot (250 mμ)

Intensities (erg/cm^2 sec)	
1.2×10^4	O
1.6×10^4	●
2.6×10^4	◐

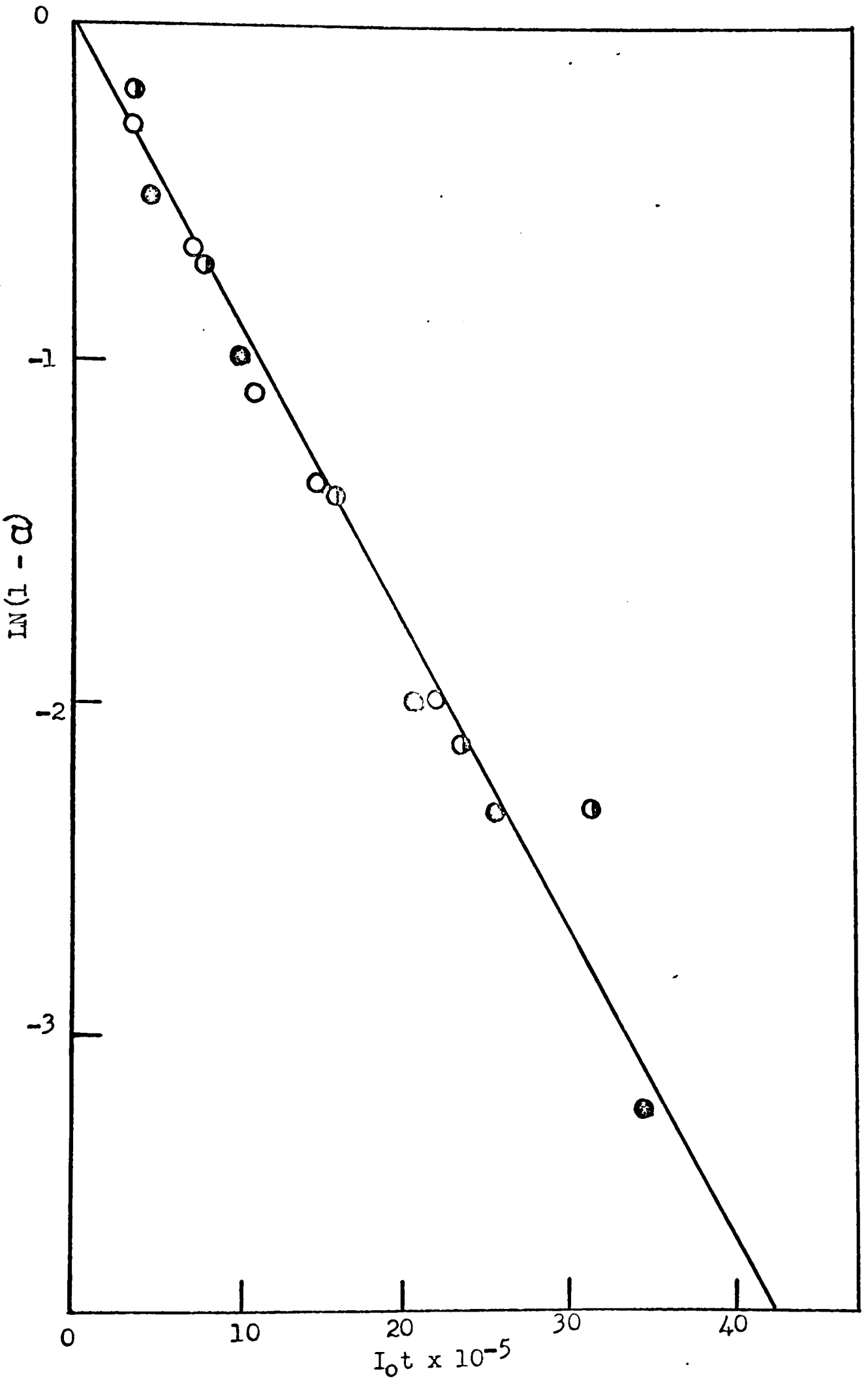
0
-1
-2
-3
LN(1 - α)
0
10
20
30
40
$I_o t \times 10^{-5}$

APPENDIX D: TABLES OF PHOTOCHEMICAL KINETIC DATA

TABLE IX

PHOTOCHEMICAL KINETIC DATA (400 mμ)

Time (min)	Fraction Reacted	$1 - \alpha$	$\ln(1 - \alpha)$
$I_o = 3.0 \times 10^4$ erg/cm^2 sec			
2	.10	.90	-.10
4	.21	.79	-.24
6	.25	.75	-.29
8	.36	.64	-.45
10	.54	.46	-.78
$I_o = 6.1 \times 10^4$ erg/cm^2 sec			
2	.14	.86	-.15
4	.25	.75	-.29
6	.38	.62	-.48
8	.44	.56	-.58
10	.52	.48	-.73
$I_o = 1.0 \times 10^5$ erg/cm^2 sec			
2	.17	.83	-.19
4	.32	.68	-.39
6	.44	.56	-.59
8	.52	.48	-.73
10	.59	.41	-.89
$I_o = 8.0 \times 10^4$ erg/cm^2 sec			
5	.29	.71	-.34
8	.44	.56	-.58
11	.56	.44	-.82
14	.64	.36	-1.02
17	.69	.31	-1.17
$I_o = 1.2 \times 10^5$ erg/cm^2 sec			
2	.19	.81	-.21
4	.36	.64	-.45
6	.50	.50	-.69
8	.60	.40	-.92
10	.68	.32	-1.14

TABLE X

PHOTOCHEMICAL KINETIC DATA (375 mμ)

Time (min)	Fraction Reacted	1 - α	ln(1 - α)
I_o = 3.7 x 10^4 erg/cm^2 sec			
4	.11	.89	-.12
8	.23	.77	-.26
12	.34	.66	-.42
16	.42	.58	-.54
20	.50	.50	-.69
I_o = 5.2 x 10^4 erg/cm^2 sec			
2	.09	.91	-.09
4	.21	.79	-.24
7	.31	.69	-.37
10	.44	.56	-.58
13	.54	.46	-.78
I_o = 7.5 x 10^4 erg/cm^2 sec			
4	.15	.85	-.16
8	.31	.69	-.37
12	.43	.57	-.56
16	.52	.48	-.73
20	.61	.39	-.94
Io = 8.6 x 10^4 erg/cm2 sec			
3	.15	.85	-.16
6	.30	.70	-.36
9	.42	.58	-.54
12	.52	.48	-.73
15	.59	.41	-.89
I_o = 1.2 x 10^5 erg/cm^2 sec			
2	.23	.77	-.26
4	.25	.75	-.29
6	.34	.66	-.42
8	.44	.56	-.58
10	.64	.36	-1.02

TABLE XI

PHOTOCHEMICAL KINETIC DATA (350 mμ)

Time (min)	Fraction Reacted	1 - α	ln(1 - α)
I_o = 3.0 x 10^4 erg/cm^2 sec			
4	.21	.79	-.23
7	.40	.60	-.51
10	.54	.46	-.79
13	.65	.35	-1.04
16	.72	.28	-1.26
I_o = 4.3 x 10^4 erg/cm^2 sec			
4	.33	.67	-.40
6	.49	.51	-.67
8	.59	.41	-.88
11	.72	.28	-1.30
13	.78	.22	-1.52
I_o = 5.6 x 10^4 erg/cm^2 sec			
2	.15	.85	-.16
4	.38	.62	-.48
6	.54	.46	-.78
8	.65	.35	-1.05
10	.74	.26	-1.35
I_o = 7.2 x 10^4 erg/cm^2 sec			
2	.23	.77	-.26
4	.50	.50	-.70
6	.68	.32	-1.14
8	.77	.23	-1.47
10	.84	.16	-1.83
I_o = 1.1 x 10^5 erg/cm^2 sec			
6	.87	.13	-2.00
8	.91	.09	-2.40
10	.94	.06	-2.81
12	.97	.03	-3.52
14	.99	.01	-4.61

TABLE XII

PHOTOCHEMICAL KINETIC DATA (325 mμ)

Time (min)	Fraction Reacted	1 - a	ln(1 - a)
$I_o = 1.0 \times 10^4$ erg/cm^2 sec			
2	.19	.81	-.19
4	.35	.65	-.40
6	.46	.54	-.70
8	.56	.44	-.92
10	.64	.36	-1.10
$I_o = 1.8 \times 10^4$ erg/cm^2 sec			
2	.30	.70	-.29
4	.51	.49	-.70
6	.65	.35	-1.15
8	.76	.24	-1.48
10	.83	.17	-1.82
$I_o = 2.7 \times 10^4$ erg/cm^2 sec			
2	.46	.54	-.71
4	.69	.31	-1.24
6	.83	.17	-1.80
8	.90	.10	-2.35
10	.96	.04	-2.90
$I_o = 4.0 \times 10^4$ erg/cm^2 sec			
2	.61	.39	-1.02
4	.85	.15	-1.88
6	.95	.05	-2.70
8	.98	.02	-3.80
10	.99	.01	-4.71
$I_o = 6.0 \times 10^4$ erg/cm^2 sec			
1	.48	.52	-.76
2	.65	.27	-1.88
3	.76	.14	-2.01
4	.83	.06	-2.60
5	.87	.02	-3.20

TABLE XIII

PHOTOCHEMICAL KINETIC DATA (300 mμ)

Time (min)	Fraction Reacted	1 - α	ln(1 - α)
$I_o = 2.9 \times 10^3$ erg/cm^2 sec			
2	.08	.92	-.10
4	.12	.88	-.14
6	.20	.80	-.25
8	.27	.73	-.34
10	.33	.67	-.41
$I_o = 8.6 \times 10^3$ erg/cm^2 sec			
3	.30	.70	-.34
7	.63	.37	-1.05
10	.75	.25	-1.60
13	.79	.21	-1.73
16	.89	.11	-2.01
$I_o = 1.1 \times 10^4$ erg/cm^2 sec			
3	.36	.64	-.37
6	.68	.32	-1.00
9	.82	.18	-1.41
12	.88	.12	-1.59
15	.92	.08	-2.05
$I_o = 1.2 \times 10^4$ erg/cm^2 sec			
2	.18	.82	-.25
4	.41	.59	-.54
6	.55	.45	-.85
8	.63	.37	-1.04
10	.73	.27	-1.36
$I_o = 1.4 \times 10^4$ erg/cm^2 sec			
2	.46	.54	-.55
5	.80	.20	-1.53
7	.88	.12	-2.24

TABLE XIV

PHOTOCHEMICAL KINETIC DATA (275 mμ)

Time (min)	Fraction Reacted	1 - α	ln(1 - α)
$I_o = 5.1 \times 10^3$ erg/cm2 sec			
2	.31	.69	-.50
4	.51	.49	-.71
6	.61	.39	-.95
8	.70	.30	-1.20
10	.75	.25	-1.39
$I_o = 8.4 \times 10^3$ erg/cm2 sec			
2	.56	.44	-.82
4	.72	.28	-1.27
6	.83	.17	-1.77
8	.91	.09	-2.40
10	.95	.05	-3.01
$I_o = 1.3 \times 10^4$ erg/cm2 sec			
2	.64	.36	-1.01
4	.83	.17	-1.75
6	.92	.08	-2.50
8	.97	.03	-3.40
10	.98	.02	-4.15
$I_o = 1.8 \times 10^4$ erg/cm2 sec			
2	.76	.24	-1.41
4	.92	.08	-2.50
6	.97	.03	-3.52
8	.99	.01	-4.75
$I_o = 2.2 \times 10^4$ erg/cm2 sec			
2	.80	.20	-1.60
4	.95	.05	-3.01
6	.99	.01	-4.75

TABLE XV

PHOTOCHEMICAL KINETIC DATA (250 mμ)

Time (min)	Fraction Reacted	1 - α	ln(1 - α)
$I_o = 1.2 \times 10^4$ erg/cm^2 sec			
30	.26	.74	-.30
60	.51	.49	-.72
90	.67	.33	-1.10
120	.76	.24	-1.42
180	.88	.12	-2.01
$I_o = 1.6 \times 10^4$ erg/cm^2 sec			
30	.33	.67	-.54
60	.64	.36	-1.00
127	.87	.13	-2.01
157	.90	.10	-2.34
217	.96	.04	-3.24
$I_o = 2.6 \times 10^4$ erg/cm^2 sec			
15	.21	.79	-.23
30	.52	.48	-.73
60	.77	.23	-1.46
90	.88	.12	-2.14
120	.90	.10	-2.34

APPENDIX E: THERMAL DATA PLOTS

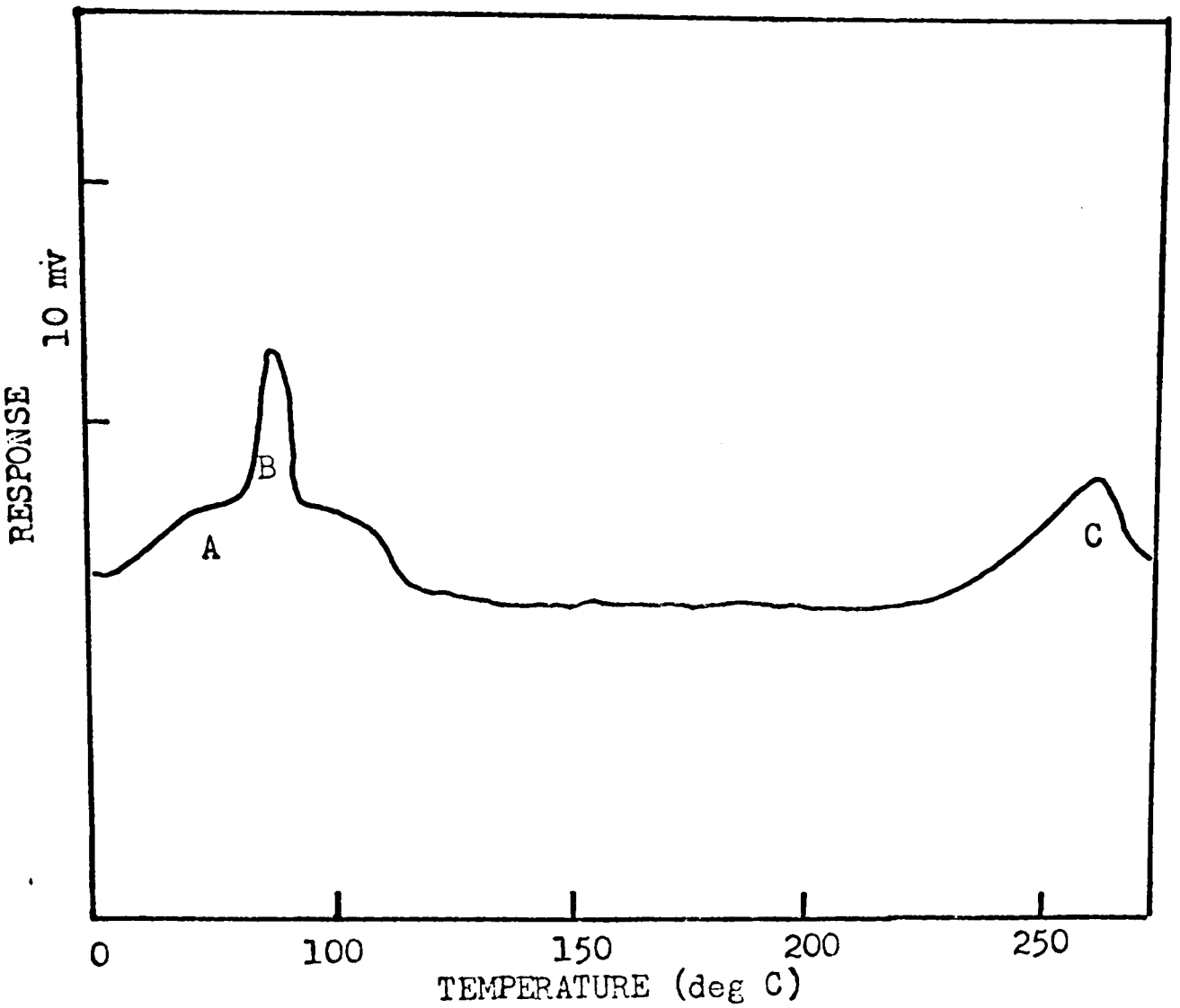

FIGURE 19

GAS EVOLUTION CURVE (22)

A. Water

B. Carbon dioxide

C. Carbon dioxide and carbon monoxide

FIGURE 20. Rate Plots of the Evolution of Water

50° C ○

57° C ◐

59° C ●

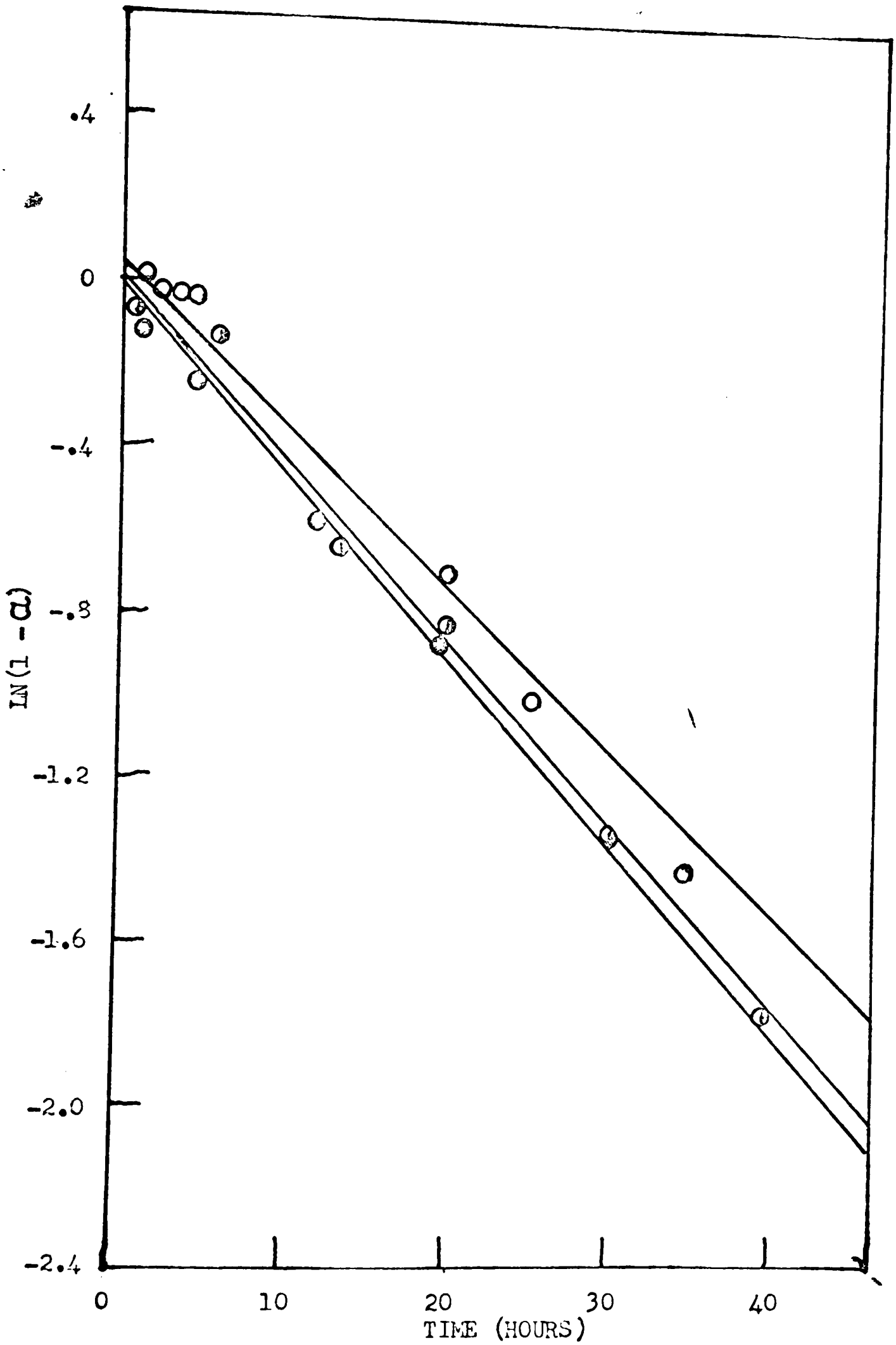
.4
0
-.4
-.8
-1.2
-1.6
-2.0
-2.4
LN(1 - α)
0
10
20
30
40
TIME (HOURS)

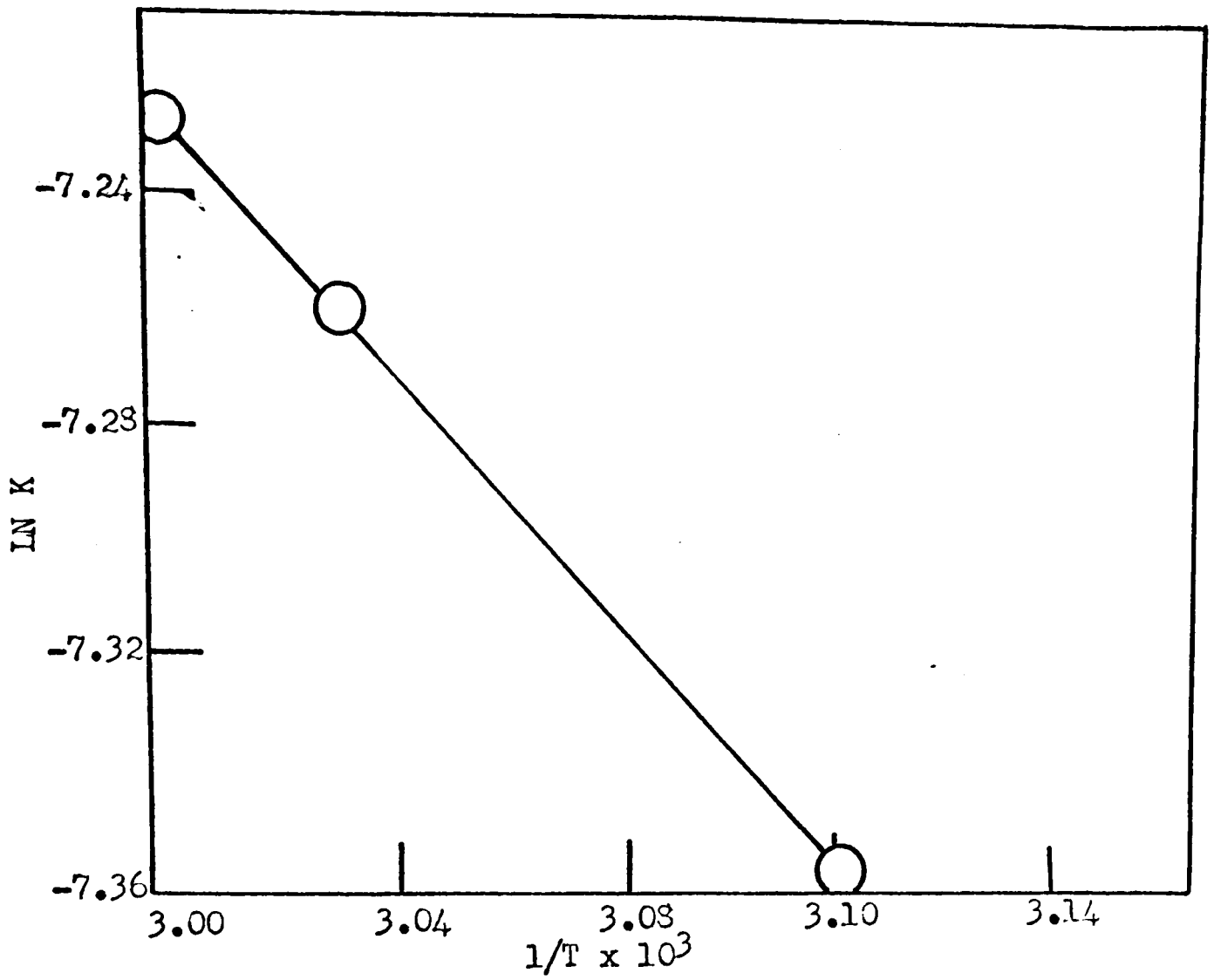

FIGURE 21

ARRHENIUS PLOT FOR THE EVOLUTION OF WATER